

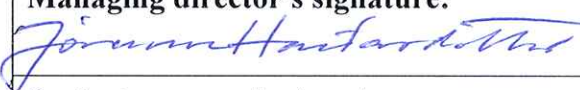
Flood frequency estimation for ungauged catchments in Iceland by combined hydrological modeling and regional frequency analysis

Philippe Crochet
Tinna Þórarinsdóttir

Flood frequency estimation for ungauged catchments in Iceland by combined hydrological modeling and regional frequency analysis

Philippe Crochet, Icelandic Met Office
Tinna Þórarinsdóttir, Icelandic Met Office

Keypage

Report no.: VÍ 2014-001	Date: May 2014	ISSN: 1670-8261	Public <input checked="" type="checkbox"/> Restricted <input type="checkbox"/> Provision:
Report title / including subtitle Flood frequency estimation for ungauged catchments in Iceland by combined hydrological modeling and regional frequency analysis		No. of copies: 20 Pages: 50 Managing director: Jórunn Harðardóttir	
Author(s): Philippe Crochet and Tinna Þórarinsdóttir		Project manager: Philippe Crochet Project number: 4812	
Project phase:		Case number: 2013-312	
Report contracted for: Vegagerðin			
Prepared in cooperation with:			
Summary: This study explores the possibility of combining hydrological modeling and a regional flood frequency analysis for estimating flood quantiles at ungauged river sites in Iceland. The idea is to first calibrate a distributed hydrological model on a gauged catchment and use it to simulate streamflow series at different ungauged sites belonging to that catchment. Subsequently, flood statistics are extracted from these simulated streamflow series and used to develop the regional flood frequency analysis which is used to infer flood quantiles at totally ungauged catchments within the same region. The method is tested in the Tröllaskagi region and the Westfjords, using hydrological simulations made with WaSiM-ETH. The results indicate that the method leads to reliable results and is capable to predict daily and instantaneous flood quantiles with reasonable accuracy for catchments with similar characteristics than those used to develop the method.			
Keywords: Iceland, flood, regional flood frequency analysis, hydrological modeling		Managing director's signature: 	
		Project manager's signature:	
		Reviewed by: Ásdís Helgadóttir and David Finger	

Contents

1	Introduction	7
2	Study area and data	8
2.1	River basins	8
2.2	Streamflow data	10
2.3	Meteorological data	10
2.4	GIS data	10
3	Index flood method	10
3.1	Principle	10
3.2	Method application using hydrological simulations	11
3.2.1	Hydrological modeling	11
3.2.2	QDF modeling	11
3.2.3	Flood frequency distribution and parameter estimation methods	12
3.2.4	Index flood method development	12
3.2.5	Index flood modeling	15
3.3	Evaluation statistics	15
4	Results	16
4.1	Daily flood quantiles	16
4.1.1	Derivation of regional growth curves	16
4.1.2	Index flood modeling and prediction	18
4.1.3	Flood quantiles prediction	19
4.2	Instantaneous flood quantiles	24
4.2.1	Derivation of regional growth curves	24
4.2.2	Index flood modeling and prediction	26
4.2.3	Flood quantiles prediction	27
5	Conclusion and future research	31
6	Acknowledgements	31
7	References	32
	Appendix I - Daily Index flood models for Region 1	35
	Appendix II - Daily Index flood models for Region 2	36
	Appendix III - Comparison between reference and estimated daily index floods for Region 1	37
	Appendix IV - Comparison between reference and estimated daily index floods for Region 2	38
	Appendix V - Empirical and modeled daily flood frequency distributions for Region 1 derived with index flood model no. 6: $\hat{\mu}(D) = a(AP/Z)^b$	39

Appendix VI - Empirical and modeled daily flood frequency distributions for Region 2 derived with index flood model no. 3: $\hat{\mu}(D) = a(APm)^b$	41
Appendix VII - Instantaneous Index flood models for Region 1.....	43
Appendix VIII - Instantaneous Index flood models for Region 2.....	44
Appendix IX - Comparison between reference and estimated instantaneous index floods for Region 1.....	45
Appendix X - Comparison between reference and estimated instantaneous index floods for Region 2.....	46
Appendix XI - Empirical and modeled instantaneous flood frequency distributions for Region 1 derived with index flood model no. 6: $\hat{\mu}(D) = a(AP/Z)^b$	47
Appendix XII - Empirical and modeled instantaneous flood frequency distributions for Region 2 derived with index flood model no. 3: $\hat{\mu}(D) = a(APm)^b$	49

1 Introduction

Flood frequency analysis is used in flood risk assessment studies and for the design of various hydraulic structures. Often, this information is required at locations where streamflow series are too short to allow a robust estimation of flood quantiles corresponding to long return periods or where no data at all are available. Regional flood frequency analysis such as the index flood method (Dalrymple 1960) offers a solution to this problem and has widely been used to estimate flood quantiles in such situations, see for instance Burn (1990), Stedinger *et al.* (1992), GREHYS (1996a, 1996b), Hosking and Wallis (1997), Jingyi and Hall (2004), Kjeldsen and D. Jones (2007), Das and Cunnane (2011), Malekinezhad *et al.* (2011a and 2011b), Zaman *et al.*, (2012) and many others. The idea is to compensate for the lack of temporal data by spatial data, taken within a region with similar flood behaviour and transfer information from gauged to ungauged sites. The underlying assumption is that flood data within a homogeneous region is drawn from the same frequency distribution, apart from a scaling factor. The method involves two major steps, i) the identification of a set of hydrologically homogeneous watersheds and ii) a regional estimation method which transfers a normalized regional flood frequency curve or growth curve at each site of interest, after proper rescaling by the so-called index flood of the target site. The index flood is often taken to be the mean of the annual maximum flood. At ungauged sites, the index flood is estimated indirectly by developing regression equations between the index flood and catchment attributes (see for instance Grover *et al.*, 2002, for a review of potential methods).

The index flood method has recently been evaluated for ten catchments in northern Iceland (Crochet, 2012a, 2012b), considering both daily and instantaneous flood quantiles. Results are promising, but the limited number of gauged sites available in these regions prevents the development of multiple regression equations for estimating the index flood. For this reason, simple regression models were developed by combining several variables together into one single explanatory variable. Results were considerably improved compared to those obtained with one single variable such as the drainage area for instance, but the limited number of gauged sites can still be an obstacle to the development of robust simple regression models. This is the most critical point towards a completely successful implementation of the method, as biased predictions of the index flood will lead to biased flood quantile predictions.

The problems encountered in estimating the index flood using indirect methods is well known and has been addressed in Brath *et al.* (2001) who acknowledged the importance and difficulties in obtaining reliable index flood estimates by indirect methods. A review of recent advances in index flood estimation was presented by Bocchiola *et al.* (2003) who suggested the use of hydrological simulations as one possible solution to indirectly infer the index flood at ungauged river sites. Continuous hydrological simulation offers an alternative approach to the index flood method for deriving flood quantiles at gauged sites with limited data availability (see for instance Blazkova and Beven, 1997; Cameron *et al.*, 1999; Fiorentino *et al.*, 2007; and a review by Boughton and Droop, 2003). A distributed hydrological model calibrated on a gauged catchment can be used to continuously simulate discharge series at different sites on that catchment and flood statistics extracted. However, the use of hydrological models to infer flood quantiles at sites located in totally ungauged catchments requires a strategy for transferring the model parameters from gauged to ungauged catchments (see for instance Post, 2009). Model complexity can be an obstacle to such a transfer approach. A solution to that problem is to perform a regional calibration (Saliha *et al.*, 2011), but this procedure requires streamflow datasets from different

sites within an homogeneous region, as for the development of the index flood method, so that the same limitations will apply regarding the robustness of the regional hydrological model, if very few gauged sites are available to perform the regional calibration.

In this study, we explore the possibility of estimating flood quantiles at ungauged catchments by combined hydrological modeling and regional frequency analysis. First, we calibrate a distributed hydrological model on a gauged catchment and use it to simulate streamflow series at different sites belonging to that catchment, where no observed streamflow data are available. Then, flood statistics are extracted from these simulated streamflow series and used to develop the index flood method which is used to infer flood quantiles at ungauged catchments within the same region. By using simulated flood data made at different ungauged locations, it is expected that index flood regression models can be developed in a more robust manner than with observations from very few gauged sites. In principle, the method could be developed for an entire region even if one site only was gauged.

The report is organized as follows. Section 2 presents the study area and data. Section 3 describes the methodology. Section 4 presents the results of the proposed approach for estimating daily and instantaneous flood quantiles at ungauged catchments. Finally, Section 5 concludes the report.

2 Study area and data

2.1 River basins

11 river catchments located in north-western and northern Iceland have been selected for this study. These two regions are characterized by a very complex topography leading to large precipitation and temperature gradients (Crochet *et al.*, 2007; Crochet and Jóhannesson, 2011) and the presence of snow during a large part of winter and spring which controls streamflow seasonality (Crochet, 2013). The topography and location of catchments is shown in Fig. 1. Table 1 summarizes the main catchment characteristics. The drainage area varies from 37 km² for the smallest to 1096 km² for the largest catchment.

Table 1. Main characteristics of river basins.

Gauging station	Name	Area (km ²)	Mean elevation (m a.s.l)	Mean annual precipitation (mm) (1971-2000)	Available period for streamflow data
vhm51	Hjaltadalsá	296	730	1711	since 1958
vhm52	Kolka	163	688	1796	1957–1988
vhm92	Bægisá	39	934	1928	since 1966
vhm10	Svartá	398	535	813	since 1932
vhm45	Vatnsdalsá	456	553	846	since 1949
vhm200	Fnjóská	1096	715	1312	since 1976
vhm19	Dynjandisá	37	529	3018	since 1956
vhm38	Þverá	43	427	1761	since 1967
vhm204	Vatnsdalsá	103	456	2937	since 1977
vhm12	Haukadalsá	167	404	1773	since 1950
vhm198	Hvalá	195	403	1971	since 1976

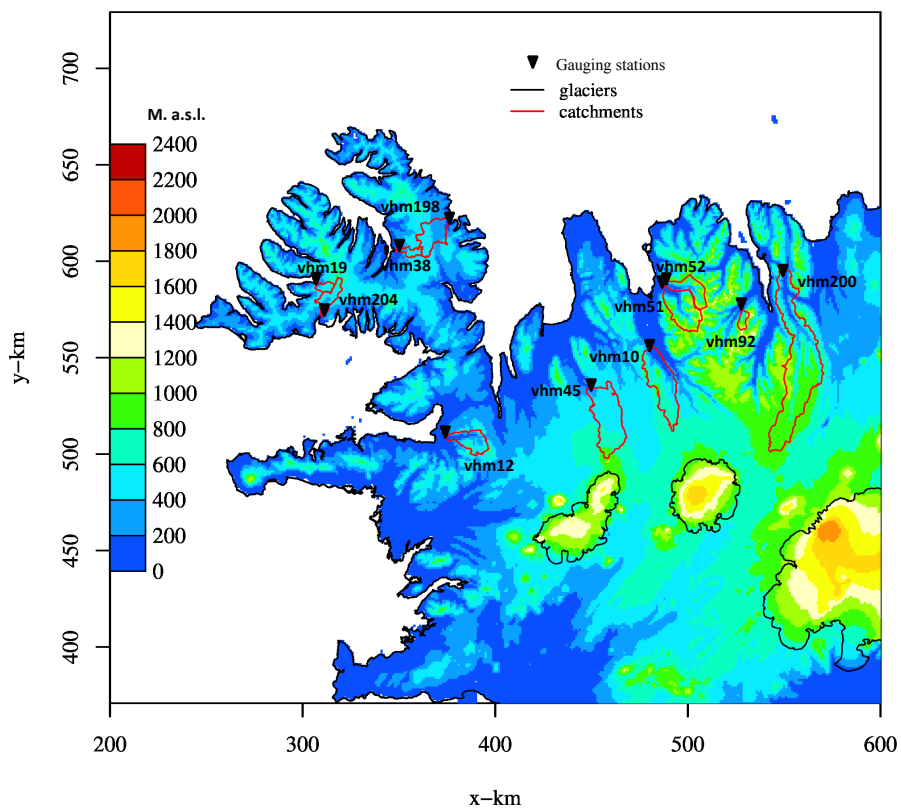


Figure 1. Topography and location of catchments.

2.2 Streamflow data

Daily discharge series and monthly maximum instantaneous discharge series were available for these catchments for variable periods. For daily flow series, annual maximum flow (AMF) series were extracted for each hydrological year (1 Sept–31 Aug), and years with more than 120 days of missing data were omitted. For instantaneous flow series, AMF series were extracted from the monthly maxima and years with more than four missing months omitted.

2.3 Meteorological data

Gridded daily precipitation (Crochet *et al.*, 2007), 2m air temperature (Crochet and Jóhannesson, 2011), 10m wind-speed, vapor pressure and incoming short wave radiation, calculated on a 1x1 km grid for the period 1961 to 2006, were used in this study to run the hydrological model and for the development of the index flood method (see below). Wind-speed, vapor pressure and incoming short wave radiation were obtained from the MM5 NWP model (Grell *et al.* 1995) at approximately 8 km resolution and interpolated to the 1x1 km grid.

2.4 GIS data

A 1 km digital elevation model derived from a 500m DEM (Icelandic Meteorological Office, National Land Survey of Iceland, Science Institute, University of Iceland, and National Energy Authority. 2004. A 500x500 m DTM of Iceland.), a soil map from the Agricultural University of Iceland and a vegetation map from the Icelandic Institute of Natural history were used in this study for describing the watersheds with the hydrological model.

3 Index flood method

3.1 Principle

The index flood method (IFM), proposed by Dalrymple (1960), is adopted here for conducting the regional flood frequency analysis and estimating flood quantiles at ungauged sites. The method has already been used in Crochet (2012a,b) and is only briefly recalled here. The idea is to estimate flood quantiles at ungauged locations using information taken from gauged sites located within the same homogeneous region. The underlying assumption is that flood data within a homogeneous region are drawn from the same frequency distribution, apart from a scaling factor. The method involves two major steps, i) the identification of a set of hydrologically homogeneous watersheds and ii) a regional estimation method for estimating the flood frequency curve at each site of interest.

Different techniques can be used to identify homogeneous groups of watersheds such as geographic proximity, or more objective methods relying on the use of catchments climatic and physiographic characteristics such as cluster analysis or the region of influence approach (Burn 1990) (see Crochet 2012b).

The regional estimation method transfers a dimensionless regional flood frequency curve or growth curve ($q_R(D, T)$) at each site of interest, after proper rescaling by the so-called index flood, $\mu_i(D)$, of the target site:

$$\widehat{Q}_i(D, T) = \mu_i(D)q_R(D, T), \quad (1)$$

where $\widehat{Q}_i(D, T)$ is the estimated flood quantile, i.e. the T -year flood peak discharge averaged over duration D , for a given site i . The mean of the AMF series for given duration D is used here to define the index flood $\mu_i(D)$. For gauged sites, $\mu_i(D)$ is estimated by the sample mean whereas for ungauged sites, $\mu_i(D)$ is estimated indirectly as a function of physiographic and climatic catchment characteristics ($C_{i,k}$):

$$\widehat{\mu}_i(D) = f(C_{i,k}), k = 1, n. \quad (2)$$

This estimation is usually performed using the power-form equation:

$$\widehat{\mu}_i(D) = \theta_0 C_{i,1}^{\theta_1} C_{i,2}^{\theta_2} \dots C_{i,k}^{\theta_k} \dots C_{i,n}^{\theta_n}. \quad (3)$$

where θ denotes the vector of model parameters. Linear regression is commonly used to infer the model parameters after logarithm transformation (see for instance Grover et al., 2002).

The regional growth curve, $q_R(D, T)$, is derived by pooling the AMF series from all gauged sites i belonging to the same region.

3.2 Method application using hydrological simulations

3.2.1 Hydrological modeling

The distributed hydrological model WaSiM-ETH (Schulla and Jasper, 2007; Atladóttir *et al.*, 2011; Þórarinsdóttir, 2012) was calibrated on 4 gauged catchments (vhm19, vhm38, vhm51 and vhm52). A semi-automatic multi-objective optimization based on the analysis of discharge information was used to assist in the selection of best model parameters for each catchment (Crochet, 2012d). The model was then used to simulate daily streamflow series at different sites within these 4 catchments. The simulated periods considered in this study are 1973-2003 for vhm19 and vhm38 and 1970-2002 for vhm51 and vhm52. The sites in question correspond to the gauging station of each catchment and to various ungauged sites, upstream of the gauging stations. The simulations were performed at 14 locations within vhm19, 13 locations within vhm38, 15 locations within vhm51 and 9 locations within vhm52. Then, flood statistics are extracted from these simulated series and used to develop the regional flood frequency analysis. According to Hoskings and Wallis (1997), unless extreme quantiles are to be estimated, there is little to be gained by using regions larger than about 20 sites in the regional frequency analysis.

3.2.2 QDF modeling

As WaSiM-ETH was used to simulate daily streamflow series, only AMF series corresponding to flow averaged over duration $D \geq 1$ day could be directly derived from the daily simulations. In order to derive instantaneous flood quantiles, $Q_i(D = 0, T)$ from these daily streamflow simulations and develop the IFM for $D = 0$, the flood-duration-frequency (QDF) model presented in Crochet (2012c) was used. This model is built on the approach proposed by Javelle *et al.* (2003):

$$Q_i(D, T) = \mu_i(D)qp_i(T), \quad (4)$$

where $Q_i(D, T)$ is the T-year flood quantile at site i , for given duration D , $\mu_i(D)$ is the index flood, as defined above, i.e. the mean of the AMF series for duration D , and $qp_i(T)$ is a dimensionless parent distribution with a mean of unity, equivalent to a growth curve. This parent distribution is estimated at each site i with the same method used to estimate $q_R(D, T)$, but instead of pooling AMF series for a given duration D from different sites, the estimation is made individually for each site i by pooling AMF series for different durations D (see Crochet, 2012c). The index flood $\mu_i(D)$, is modeled at each site i as a continuous function of D , as follows:

$$\mu_i(D) = \frac{\mu_i}{1 + (D/\Delta_i)^{\lambda_i}}, \quad (5)$$

where μ_i , Δ_i and λ_i are basin dependent parameters that have to be calibrated. The parameter μ_i corresponds to the mean instantaneous ($D = 0$) AMF which is also the instantaneous index flood in this study. Details of the optimal estimation of model parameters Δ_i , μ_i and λ_i are described in Crochet (2012c). Note that in the original formulation proposed by Javelle *et al.* (2003), only μ_i and Δ_i are defined, which is equivalent to have $\lambda_i = 1$. In this study, $0.5 \leq \lambda_i \leq 1$. A regional growth curve, $q_R(D, T)$, is then derived from the parent distributions $qp_i(T)$ obtained at all sites i belonging to the same region.

Once $\mu_i(D)$ and $q_R(D, T)$ are known for $D = 0$, the index flood method can be developed to infer instantaneous flood quantiles at ungauged sites, as described in Section 3.1.

3.2.3 Flood frequency distribution and parameter estimation methods

The Generalized Extreme Value (GEV) distribution (Jenkinson, 1955) is adopted to model the flood frequency distribution at each site, from the AMF series:

$$Q_i(D, T) = \begin{cases} \varepsilon_i + \frac{\alpha_i}{\kappa_i} (1 - [-\ln(1 - 1/T)]^{\kappa_i}) & \text{if } \kappa_i \neq 0 \\ \varepsilon_i - \alpha_i \ln(-\ln(1 - 1/T)) & \text{if } \kappa_i = 0 \end{cases} \quad (6)$$

where ε_i is the location parameter, α_i is the scale parameter and κ_i is the shape parameter. The method of probability weighted moments (PWM) proposed by Hosking *et al.* (1985a) is adopted to fit the individual GEV distributions at each site and the parameters of the regional growth curve ($q_R(D, T)$) are estimated with the GEV/PWM regionalization algorithm proposed by Hosking *et al.* (1985b).

3.2.4 Index flood method development

Two regions were defined for the development of the index flood method (as in Crochet 2012a,b):

- Region 1: vhm51, vhm52, vhm92, vhm10, vhm45 and vhm200
- Region 2: vhm19, vhm38, vhm12, vhm204 and vhm198

To evaluate the performance of the index flood method at ungauged sites, a cross validation approach was adopted. Figure 2 summarizes the methodology. For each region, the streamflow series simulated with WaSiM-ETH at all defined sites within a given catchment were used to develop the index flood method (i.e. the regional growth curve $q_R(D, T)$ and the regression equations predicting the index flood $\mu_i(D)$ (Eq. 3)). This information was used to estimate daily and instantaneous flood quantiles at the other gauged sites belonging to the same region, assuming that they were ungauged. Reference and estimated flood quantiles were compared. This gives two sets of estimates for each region, as follows:

- For Region 1, the regional growth curve, $q_R(D, T)$, and index flood models were first developed using streamflow simulations made at the 15 sites within catchment vhm51. This information was used to estimate flood quantiles at gauging sites vhm52, vhm92, vhm10, vhm45 and vhm200. Then, the regional growth curve and index flood models were developed using streamflow simulations made at the 9 sites within catchment vhm52. This information was used to estimate flood quantiles at gauging sites vhm51, vhm92, vhm10, vhm45 and vhm200.
- For Region 2, the regional growth curve and index flood models were first developed using streamflow simulations made at the 14 sites within catchment vhm19. This information was used to estimate flood quantiles at gauging sites vhm38, vhm12, vhm204 and vhm198. Then, the regional growth curve and index flood models were developed using streamflow simulations made at the 13 sites within catchment vhm38. This information was used to estimate flood quantiles at gauging sites vhm19, vhm12, vhm204 and vhm198.
- Reference flood quantiles were derived from the GEV distribution fitted to the observed AMF series at each gauged site and compared to the estimated ones derived with the IFM. The GEV distribution was also fitted directly to the simulations made with WaSiM-ETH at gauged sites vhm19, vhm38, vhm51 and vhm52 for comparison with the reference quantiles derived from observations.

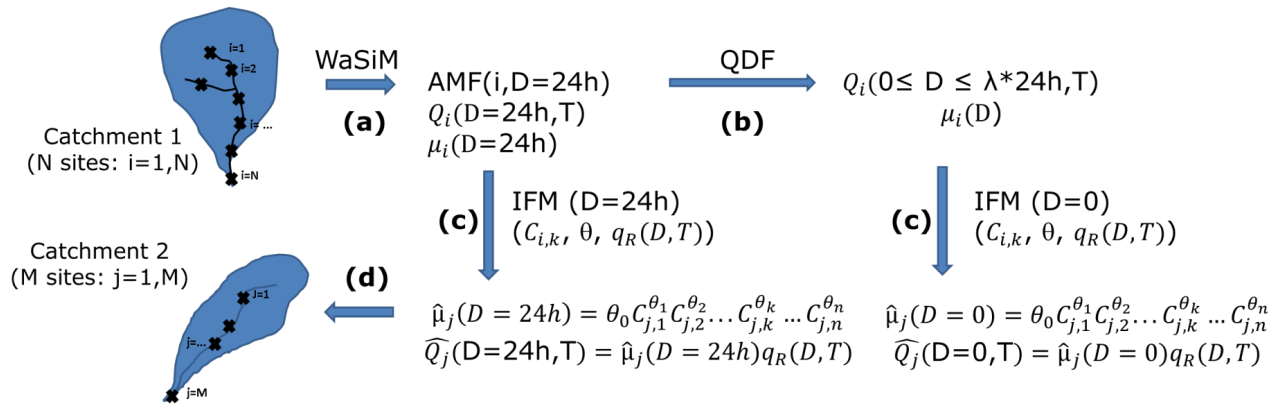


Figure 2. Method flow chart. Daily ($D = 24h$) AMF series simulated with WaSiM-ETH at all defined sites within a given catchment were extracted (a) and daily flood quantiles and index floods calculated. A Flood-Duration-Frequency (QDF) model was applied to derive instantaneous ($D = 0$) flood quantiles and index floods (b). This information was then used to develop the IFM (c), i.e. the regional growth curve, $q_R(D, T)$, and the index flood model parameters (θ). This information was used to estimate daily and instantaneous flood quantiles at the other gauged sites belonging to the same region, assuming that they were ungauged (d).

3.2.5 Index flood modeling

In order to estimate the index flood, $\mu_i(D)$, at ungauged sites, for a given duration D , several relationships between $\mu_i(D)$ and various physiographic and climatic catchment characteristics were developed using simulated streamflow series made with WaSiM-ETH. These relationships were developed for daily and instantaneous index floods. Several models were tested and their parameters estimated by ordinary least square regression after logarithm transformation:

$$\hat{\mu}_i(D) = a(A_i)^b \quad (7)$$

$$\hat{\mu}_i(D) = a(A_i/L_i)^b \quad (8)$$

$$\hat{\mu}_i(D) = a(A_i P_{mi})^b \quad (9)$$

$$\hat{\mu}_i(D) = a(A_i P_i)^b \quad (10)$$

$$\hat{\mu}_i(D) = a(A_i P_{mi}/Z_i)^b \quad (11)$$

$$\hat{\mu}_i(D) = a(A_i P_i/Z_i)^b \quad (12)$$

Where $\theta = (a, b)$ is the vector of regression parameters, A is the drainage area in km^2 , L the catchment perimeter in km, Z the catchment mean altitude in meters, P the catchment averaged mean annual precipitation in mm/day for the period 1971–2000 and P_m the catchment averaged mean annual maximum daily precipitation in mm/day for the period 1971–2000.

3.3 Evaluation statistics

The evaluation of the index flood regression models (Eqs. 7 to 12) was first conducted by calculating the coefficient of determination (R^2). Then, the ability of each model to predict the index flood, $\hat{\mu}_i(D)$, at ungauged sites was evaluated by calculating the root mean squared error (RMSE) between reference and estimated index floods. The reference index flood was derived from real observations at gauged sites and from simulated series, not used to develop the regression equations.

Reference and predicted flood quantiles were compared at gauged sites only, treated as ungauged, for average recurrence intervals T of 2, 5, 10, 20, 50 and 100 years. The performance of the prediction was evaluated by cross-validation at independent sites not used in the method development, by calculating the mean relative error ($BIAS_T$) and relative root mean squared error ($RMSE_T$):

$$BIAS_T(\%) = \frac{1}{N} \sum_{i=1}^N \frac{1}{L} \sum_{l=1}^L \left(\frac{Q_i(D, T_l) - \hat{Q}_i(D, T_l)}{Q_i(D, T_l)} \right) \times 100, \quad (13)$$

$$RMSE_T(\%) = \frac{1}{N} \sum_{i=1}^N \sqrt{\frac{1}{L} \sum_{l=1}^L \left(\frac{Q_i(D, T_l) - \hat{Q}_i(D, T_l)}{Q_i(D, T_l)} \right)^2} \times 100, \quad (14)$$

where $Q_i(D, T_l)$ is the reference flood quantile at gauged site i and return period T_l , calculated with the GEV distribution from the observed AMF series and $\hat{Q}_i(D, T_l)$ is the estimated flood quantile, calculated with the index flood method, (Eq. 1).

4 Results

4.1 Daily flood quantiles

This section presents the results of the regional flood frequency analysis developed with daily ($D = 24\text{h}$) AMF series simulated with WaSiM-ETH.

4.1.1 Derivation of regional growth curves

Figures 3 and 4 present the individual growth curves calculated at each gauged site within each region with the observed streamflow series, and the regional growth curves derived from the streamflow simulations made at different sites within catchments vhm51, vhm52, vhm19 and vhm38 respectively. These growth curves superimpose quite well. The H -statistics (Hoskings and Wallis, 1993, 1997) are also given. According to this test, a region is acceptably homogeneous if $H < 1$, possibly heterogeneous if $1 \leq H < 2$ and definitely heterogeneous if $H \geq 2$.

The H -statistics calculated with the observed AMF series indicate that the two regions are homogeneous, although Region 1 could be slightly heterogeneous. When the H -statistics are calculated with the simulated AMF series within each catchment, the values are negative, indicating the presence of positive cross-correlation between the different sites frequency distributions or an excessive regularity in the data (Hoskings and Wallis, 1997). This was expected as the different sites within the same catchment where streamflow series have been simulated are close to one another. The main effect of intersite dependence is to increase the variability of estimators, acting similarly to a reduction in the number of sites in the region (Hoskings and Wallis, 1997). However, according to these authors, small amount of intersite dependence should not be a concern in regional estimation and regionalization is valuable even with moderate amount of heterogeneity, intersite dependence and misspecification of the frequency distribution.

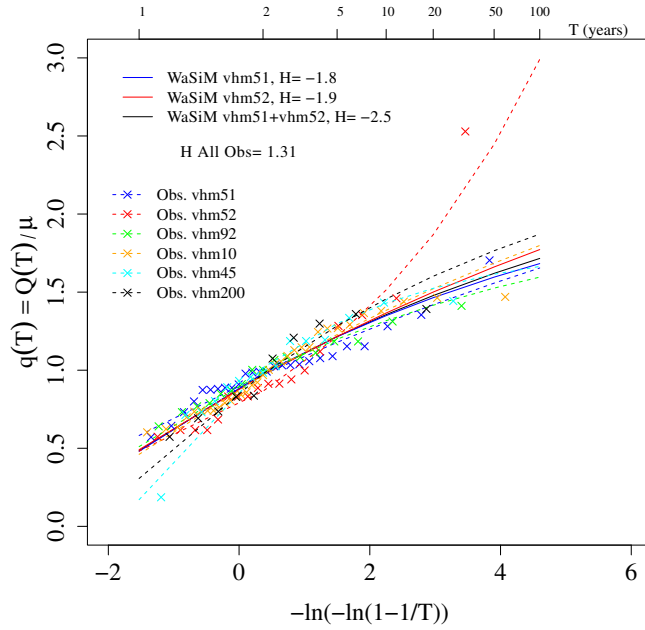


Figure 3. Daily AMF series: Regional growth curves ($q_R(D, T)$) for Region 1 (solid lines) calculated from WaSiM simulations within catchments vhm51 and vhm52 and individual growth curves at each gauged catchment ($q_i(D, T) = Q_i(D, T)/\mu_i(D)$) derived from observed AMF series (dashed lines).

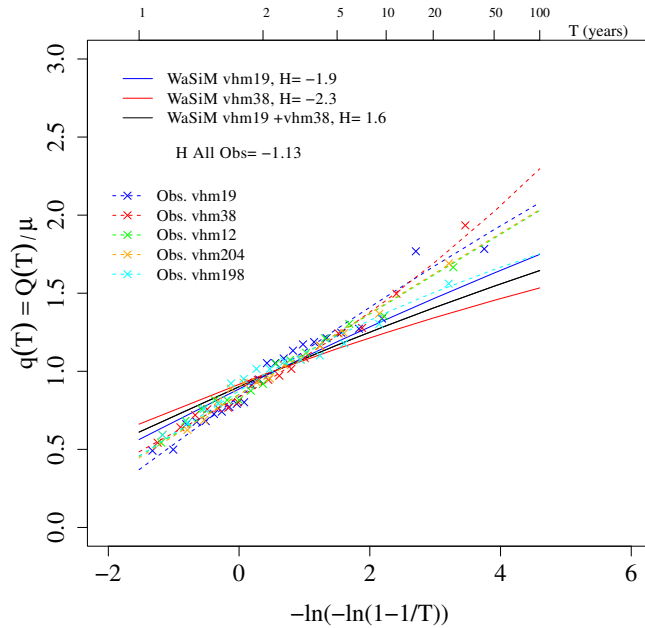


Figure 4. Daily AMF series: Regional growth curves ($q_R(D, T)$) for Region 2 (solid lines) calculated from WaSiM simulations within catchments vhm19 and vhm38 and individual growth curves at each gauged catchment ($q_i(D, T) = Q_i(D, T)/\mu_i(D)$) derived from observed AMF series (dashed lines).

4.1.2 Index flood modeling and prediction

Appendices I to IV present the results of the modeling of the index flood ($\mu_i(D)$) as a function of catchment characteristics, for the two regions, considering the 6 models (Eqs. 7 to 12). Appendices I and II present the linear regressions between $\mu_i(D)$ and catchment characteristics. Appendices III and IV present the cross-validation, i.e. the comparison between reference and estimated index flood at independent gauged and simulated sites, not used in the development of the index flood models (see flowchart in Fig. 2). Tables 2 and 3 summarize the results.

The best index flood model is different for the two regions. When the validation is conducted at simulated sites only, model no. 6 gives the best results for Region 1 and models no. 3 and 4 give the best results for Region 2. When the validation is conducted at all independent gauged sites of each region with observed AMF series, the best results are obtained with models no. 1 and 3 for Region 1 and with model no. 6 for Region 2.

Note also that in each region, the pairs of catchments used to develop and validate the index flood models with simulated series are of relatively similar size, while some of the other catchments are much larger, and so is their index flood. Consequently, the RMSE obtained when validating the method with the simulated series are usually lower than those obtained with the observed series from the other catchments.

When the best index flood model is considered for each region, results of this analysis indicate that $\mu_i(D)$ is correctly estimated for catchments whose characteristics are similar to those used to develop the index flood models. On the other hand, the estimation of $\mu_i(D)$ is very uncertain for catchments whose characteristics are very different than those used to develop the index flood models. This is the case for the largest ones. For these catchments, the index flood model is extrapolated far beyond the range of characteristics for which it was developed and the estimation of $\mu_i(D)$ may not be valid. This is in line with Crochet (2012a,b). This is the case in Region 1 for catchment vhm200, for which the index flood is usually strongly underestimated. This catchment is by far the largest and much larger than vhm51 and vhm52, used to develop the index flood models. In that region, model no. 1 seems to perform better than the other models, only because it gives a better estimate for vhm200 which has the largest index flood. However, the index flood prediction at the other catchments with model no. 1 is not better than with the other models. In Region 2, the two catchments used to develop the index flood models (vhm19 and vhm38) are the smallest of the region. The index flood $\mu_i(D)$ is well predicted at the three smallest catchments and poorly predicted at the two largest ones, vhm12 and vhm198, for the same reasons mentioned above.

Table 2. Daily index flood modeling. R^2 score from the regression equations developed within each catchment with simulated series. Catchments used in the development of regression equations are indicated in brackets.

model	1 $\hat{\mu}_i(D) = a(A_i)^b$	2 $\hat{\mu}_i(D) = a(A_i/L_i)^b$	3 $\hat{\mu}_i(D) = a(A_iP_{mi})^b$	4 $\hat{\mu}_i(D) = a(A_iP_i)^b$	5 $\hat{\mu}_i(D) = a(A_iP_{mi}/Z_i)^b$	6 $\hat{\mu}_i(D) = a(A_iP_i/Z_i)^b$
Region 1 (vhm51)	0.983	0.979	0.993	0.993	0.976	0.976
Region 1 (vhm52)	0.957	0.977	0.974	0.977	0.934	0.939
Region 2 (vhm19)	0.957	0.906	0.959	0.963	0.955	0.96
Region 2 (vhm38)	0.956	0.972	0.966	0.972	0.952	0.959

Table 3. Validation of the daily index flood predictions at gauged and simulated sites, treated as ungauged. RMSE scores (m^3/s) calculated at simulated sites (WaSiM) and gauged sites (Obs). For the gauged sites, RMSE is first calculated for each of the two sets of estimates and then averaged (see Table 2, Appendices III and IV, and Section 3.2.4).

model	1 $\hat{\mu}_i(D) = a(A_i)^b$	2 $\hat{\mu}_i(D) = a(A_i/L_i)^b$	3 $\hat{\mu}_i(D) = a(A_iP_{mi})^b$	4 $\hat{\mu}_i(D) = a(A_iP_i)^b$	5 $\hat{\mu}_i(D) = a(A_iP_{mi}/Z_i)^b$	6 $\hat{\mu}_i(D) = a(A_iP_i/Z_i)^b$
Region 1 (WaSiM)	7.4	7.8	6.6	5.6	5.4	4.7
Region 1 (Obs)	29.4	79.1	29.7	40.2	34	40.4
Region 2 (WaSiM)	7.1	3.5	1.4	1.5	3.2	2.3
Region 2 (Obs)	21.5	25.5	21.8	19	19.7	16.2

4.1.3 Flood quantiles prediction

Figures 5 and 6 present the mean relative error ($BIAS_T$) and relative RMSE ($RMSE_T$) calculated on 4 quantiles ($T=2, 5, 10$ and 50 years) and summarize the overall quality of the estimated daily flood quantiles at ungauged sites for the two regions.

The prediction error depends on the quality of i) the hydrological simulations, ii) the index flood prediction models and iii) the regional growth curve at the site in question. As a consequence, the best results are not systematically obtained with the index flood model giving the lowest RMSE (see Table 3 for a comparison), because of compensating errors such as an over- (under-) estimation of the regional growth factor and an under- (over-) estimation of the index flood. However, the dominating source of error is often the quality of the index flood prediction. The best overall results according to the $RMSE_T$ score are obtained with index flood model no. 6 for Region 1 and models no. 3 and 4 for Region 2, depending which catchment was used to develop the models. When these models are used, the predictions are relatively unbiased in average in each region and $RMSE_T$ does not exceed 25% of the reference quantiles.

Figures 7 and 8 present the reference and predicted flood frequency distributions obtained for gauged sites vhm51 and vhm52 with index flood model no. 6 and for gauged sites vhm19 and vhm38 with index flood model no. 3. Appendices V and VI present the results obtained for the other gauged sites with the same index flood models. In these figures, the confidence intervals of the IFM-based flood quantiles are derived assuming that the hydrological simulations are

perfect (see Crochet, 2012a for the modeling of the quantile uncertainty), and the uncertainty of the hydrological modeling is not included.

The predicted flood quantiles are usually within the 95% confidence interval of the reference quantiles, but poor quantiles predictions are obtained for vhm200 and vhm198. As mentioned above, these catchments are much larger than the ones used to develop the index flood models and consequently far beyond the applicability of the index flood method as developed in the present study with vhm51, vhm52, vhm19 and vhm38.

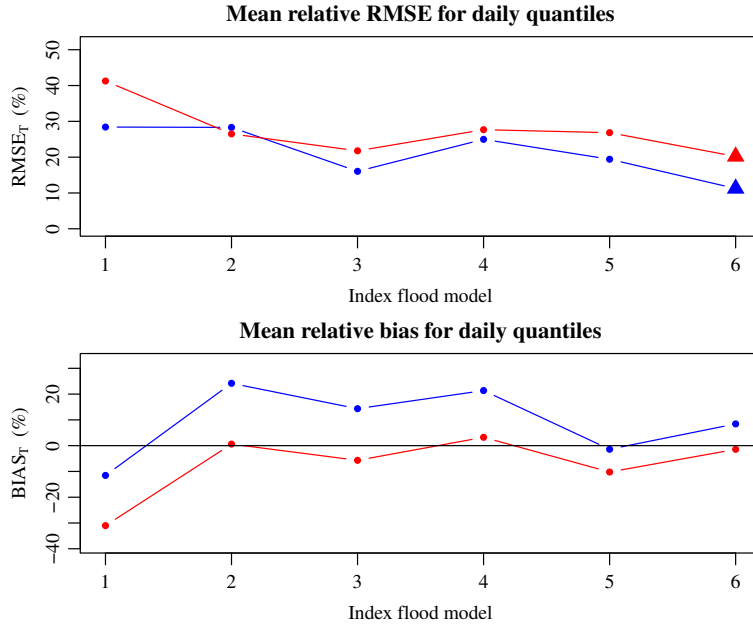


Figure 5. Daily flood quantiles at gauged sites: mean relative RMSE ($RMSE_T$) (top) and bias ($BIAS_T$) (bottom) for Region 1. The solid blue and red lines correspond to results obtained with the index flood method developed with WaSiM simulations within catchments vhm51 and vhm52, respectively. Best model with respect to $RMSE_T$ is indicated by large symbol.

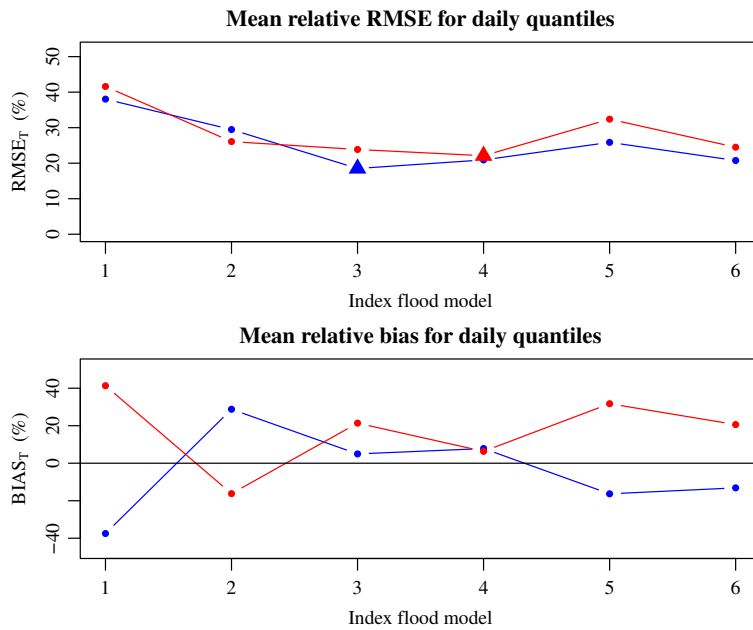


Figure 6. As Figure 5 but for Region 2. The solid blue and red lines correspond to results obtained with the index flood method developed with WaSiM simulations within catchments vhm19 and vhm38, respectively.

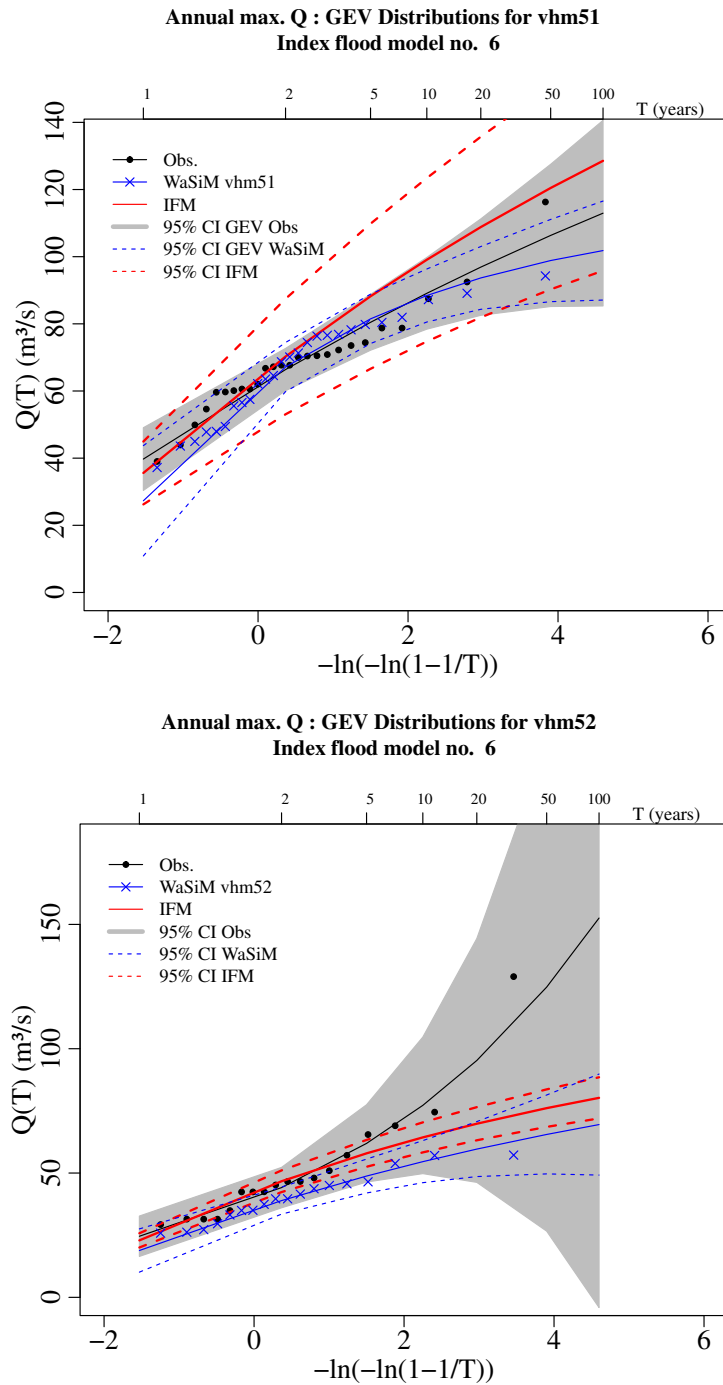


Figure 7. Region 1: Empirical and modeled daily flood frequency distributions ($Q(D,T)$) at gauged sites vhm51 (top) and vhm52 (bottom). The solid black line corresponds to the reference GEV distribution derived from the observed AMF series. The solid blue line corresponds to the GEV distribution derived from the simulated AMF series made with WaSiM, at the gauged sites. The solid red line corresponds to the distribution estimated with the IFM (Eqs. 1 and 12) developed with WaSiM simulations within vhm52 (top) and vhm51 (bottom). Dashed lines and shaded grey region correspond to the 95% confidence intervals (CI) (see Crochet 2012a). Uncertainty related to hydrological modeling is not included in the CI calculations (CI WaSiM and CI IFM in figures legend).

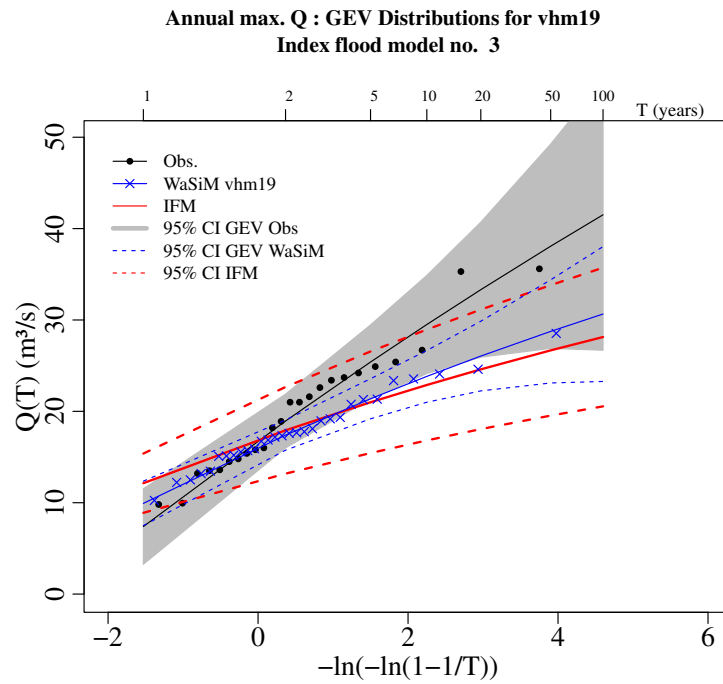


Figure 8. As for Fig. 7 but for catchments vhm19 (top) and vhm38 (bottom), located in Region 2. The solid red line corresponds to the distribution estimated with the IFM (Eqs. 1 and 9) developed with WaSiM simulations within vhm38 (top) and vhm19 (bottom).

4.2 Instantaneous flood quantiles

This section presents the results of the regional flood frequency analysis developed to infer instantaneous flood quantiles, after applying a QDF model to daily streamflow simulations made with WaSiM-ETH (see flowchart in Fig. 2). In practise, we used $D = 1$ min rather than $D = 0$ to derive instantaneous flood quantiles from streamflow simulations with the QDF model (Eqs. 4 and 5), as some of the observed instantaneous AMF series are not strictly speaking instantaneous but averaged over 1 min. However, in the rest of the text, we will keep using $D = 0$ to refer to instantaneous flood statistics.

4.2.1 Derivation of regional growth curves

Figures 9 and 10 present the individual growth curves for each gauged site derived from the observed AMF series and the regional growth curves derived from WaSiM-ETH simulations and QDF modeling at different sites within catchments vhm51, vhm52, vhm19 and vhm38 respectively. According to the H -statistics, Region 1 is heterogeneous with respect to instantaneous floods while this was not the case for daily floods. If vhm51 is removed from the group of catchments, $H=0.64$. If vhm51 and vhm52 only are combined, $H=2.7$, which would indicate that vhm51 and vhm52 do not constitute a homogeneous group while these two catchments are right next to each other in a similar physiographic and climatic environment. This heterogeneity could be related to outliers and uncertainties in the conversion of the most extreme water levels into instantaneous discharge with the rating curves. According to Hoskings and Wallis (1997), regionalization is valuable even in regions with moderate amounts of heterogeneity, intersite dependence and misspecification of the frequency distributions. According to these authors, regional estimation remains preferable for the most extreme quantiles even in regions for which the H value is considerably larger than 2. They also suggested that the criteria $H \geq 2$ for declaring a region to be definitely heterogeneous might be too strict.

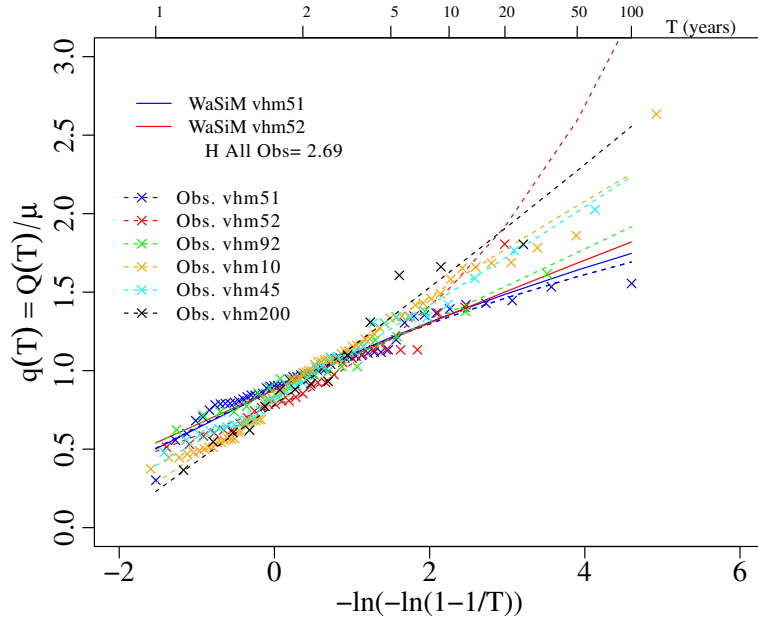


Figure 9. Instantaneous AMF series: Regional growth curves ($q_R(D, T)$) for Region 1 (solid lines) calculated from WaSiM simulations and QDF modeling within catchments vhm51 and vhm52, and individual growth curves at each gauged catchment ($q_i(D, T) = Q_i(D, T)/\mu_i(D)$) derived from observed AMF series (dashed lines).

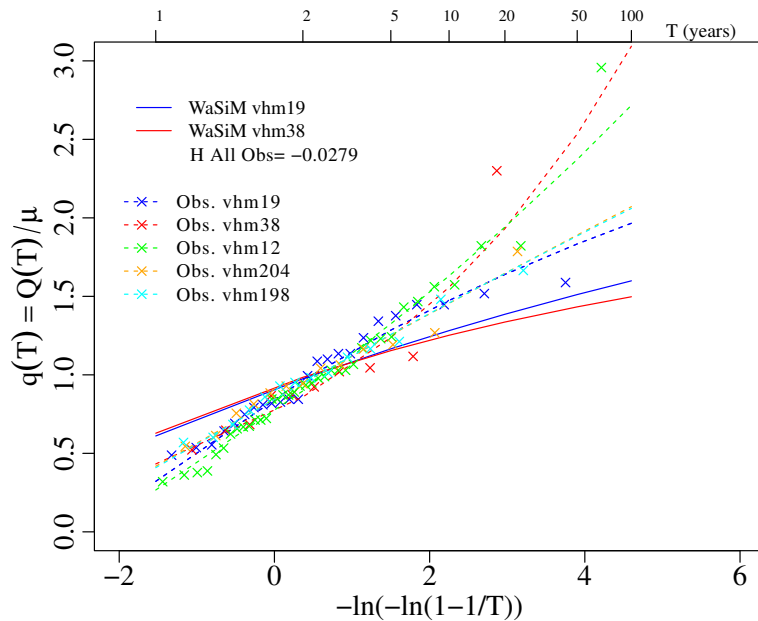


Figure 10. Instantaneous AMF series: Regional growth curves ($q_R(D, T)$) for Region 2 (solid lines) calculated from WaSiM simulations and QDF modeling within catchments vhm19 and vhm38, and individual growth curves at each gauged catchment ($q_i(D, T) = Q_i(D, T)/\mu_i(D)$) derived from observed AMF series (dashed lines).

4.2.2 Index flood modeling and prediction

Appendices VII to X present the results of the modeling of the instantaneous index flood ($\mu_i(D)$) as a function of catchment characteristics, for the two regions, after QDF modeling of the simulated AMF series at each site (not shown). Appendices VII and VIII present the linear regressions and Appendices IX and X the cross-validation, i.e. the comparison between reference and estimated index flood at independent gauged and simulated sites, not used in the development of the index flood models. Tables 4 and 5 summarize the results.

As for the daily case, the regression model giving the best instantaneous index flood predictions is different for the two regions. When the cross-validation is conducted at simulated sites only, model no. 4 gives the best results for both regions. When the cross-validation is made at all independent gauged sites of each region with observed AMF series, the best results are obtained with model no. 3 for Region 1 and with model no. 6 for Region 2, as for daily floods.

Surprisingly, relatively unbiased estimates of $\mu_i(D)$ are obtained for vhm200 with several models (see Appendix IX), while most models led to strong biased estimates at this site for the daily index flood. For Region 2, $\mu_i(D)$ is more biased on the largest catchments (vhm12 and vhm198), especially vhm198, as expected. As mentioned earlier, these results indicate that it is uncertain to estimate $\mu_i(D)$ for catchments much larger than those for which the index flood models were developed. However, considering the complexity of the modeling chain (Fig. 2), the index flood predictions with models no. 3, 4 and 6 are remarkable for catchments whose drainage area is within acceptable limits according to the regression equations (vhm19, vhm38, vhm204, vhm51, vhm52, vhm92, vhm10, vhm45).

Table 4. Instantaneous index flood modeling. R^2 score from the regression equations developed within each catchment with simulated series. Catchments used in the development of regression equations are indicated in brackets.

model	1 $\hat{\mu}_i(D) = a(A_i)^b$	2 $\hat{\mu}_i(D) = a(A_i/L_i)^b$	3 $\hat{\mu}_i(D) = a(A_i P_{mi})^b$	4 $\hat{\mu}_i(D) = a(A_i P_i)^b$	5 $\hat{\mu}_i(D) = a(A_i P_{mi}/Z_i)^b$	6 $\hat{\mu}_i(D) = a(A_i P_i/Z_i)^b$
Region 1 (vhm51)	0.967	0.966	0.982	0.982	0.959	0.959
Region 1 (vhm52)	0.939	0.984	0.959	0.963	0.913	0.918
Region 2 (vhm19)	0.977	0.931	0.978	0.982	0.975	0.979
Region 2 (vhm38)	0.957	0.971	0.966	0.973	0.953	0.96

Table 5. Instantaneous index flood estimation. Validation at gauged and simulated sites treated as ungauged. RMSE scores (m^3/s) calculated at simulated sites (WaSiM) and gauged sites (Obs). For the gauged sites, RMSE is first calculated for each of the two sets of estimates and then averaged (see Table 4, Appendices IX and X, and Section 3.2.4).

model	1	2	3	4	5	6
	$\hat{\mu}_i(D) = a(A_i)^b$	$\hat{\mu}_i(D) = a(A_i/L_i)^b$	$\hat{\mu}_i(D) = a(A_iP_{mi})^b$	$\hat{\mu}_i(D) = a(A_iP_i)^b$	$\hat{\mu}_i(D) = a(A_iP_{mi}/Z_i)^b$	$\hat{\mu}_i(D) = a(A_iP_i/Z_i)^b$
Region 1 (WaSiM)	6.83	7.2	5.75	4.77	5.94	5.55
Region 1 (Obs)	34.15	66.3	15	20.8	27.3	21.5
Region 2 (WaSiM)	7.89	3.56	2.22	1.46	4.87	3.64
Region 2 (Obs)	27.8	36.6	24.6	19.8	24.6	17.9

4.2.3 Flood quantiles prediction

In order to evaluate the methodology at ungauged catchments, the same cross-validation methodology used with daily floods was employed. Figures 11 and 12 present the mean relative bias ($BIAS_T$) and relative RMSE ($RMSE_T$) which summarize the overall quality of the estimated instantaneous flood quantiles at ungauged sites for the two regions.

The prediction error depends on the quality of i) the hydrological simulations ii) the QDF modeling, iii) the index flood prediction models and iv) the regional growth curve at the site in question. Although the dominating source of error is often the quality of the index flood prediction, the best results are not systematically obtained with the index flood model giving the lowest RMSE (see Table 5 for a comparison), because of compensating errors such as an over- (under-) estimation of the regional growth factor and an under- (over-) estimation of the index flood. The best overall results according to $RMSE_T$ are obtained with model no. 6 for Region 1 and model no. 3 for Region 2, as for the daily flood quantiles. When these models are used, the predictions are relatively unbiased in average in each region and $RMSE_T$ is between 20 and 30% of the reference quantiles, which is quite remarkable considering the complexity of the modeling chain.

Figures 13 and 14 present the reference and predicted instantaneous flood frequency distributions obtained for gauged sites vhm51 and vhm52 with model no. 6 and for gauged sites vhm19 and vhm38 with model no. 3. Appendices XI and XII present the results obtained for the other gauged sites with the same index flood models. In these figures, the confidence intervals of the IFM-based flood quantiles are derived assuming that the hydrological simulations are perfect (see Crochet, 2012a), and the uncertainties of the hydrological modeling and the QDF modeling are not included.

The predicted instantaneous flood quantiles are usually within the 95% confidence interval of the reference quantiles for the catchments whose drainage areas are within the range of drainage areas used to develop the index flood models. Poor predictions are obtained for the largest ones, namely vhm198 and vhm200. As mentioned above, this is because these catchments are much larger than the ones used to develop the index flood models and consequently far beyond the applicability of the method developed with catchments vhm51 and vhm52 for Region 1 and vhm19 and vhm38 for Region 2.

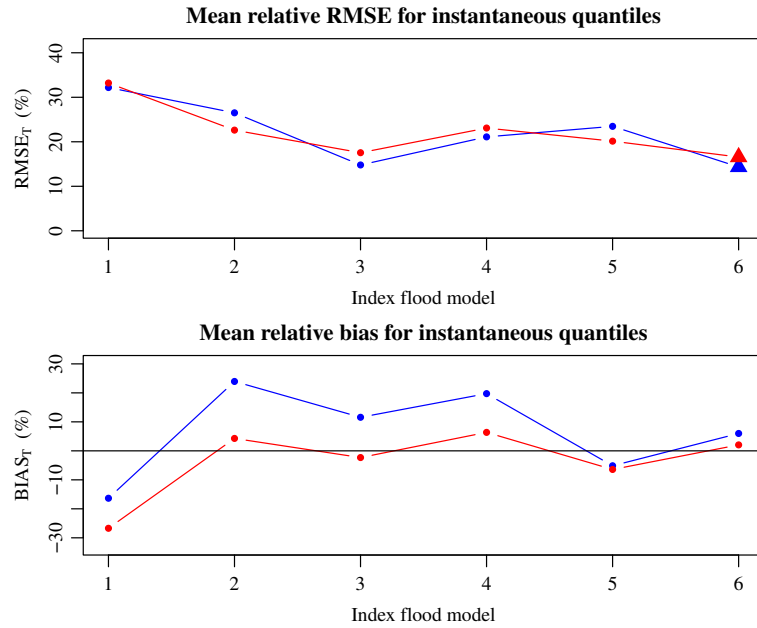


Figure 11. Instantaneous flood quantiles at gauged sites: mean relative RMSE ($RMSE_T$) (top) and bias ($BIAS_T$) (bottom) for Region 1. The solid blue and red lines correspond to results obtained with the index flood method developed with WaSiM simulations and QDF modeling within catchments vhm51 and vhm52, respectively. Best model with respect to $RMSE_T$ is indicated by large symbol.

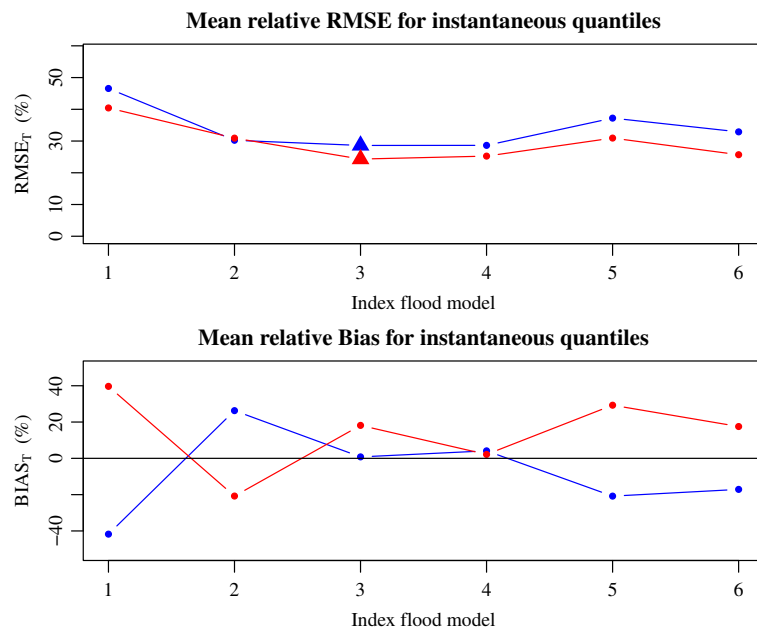
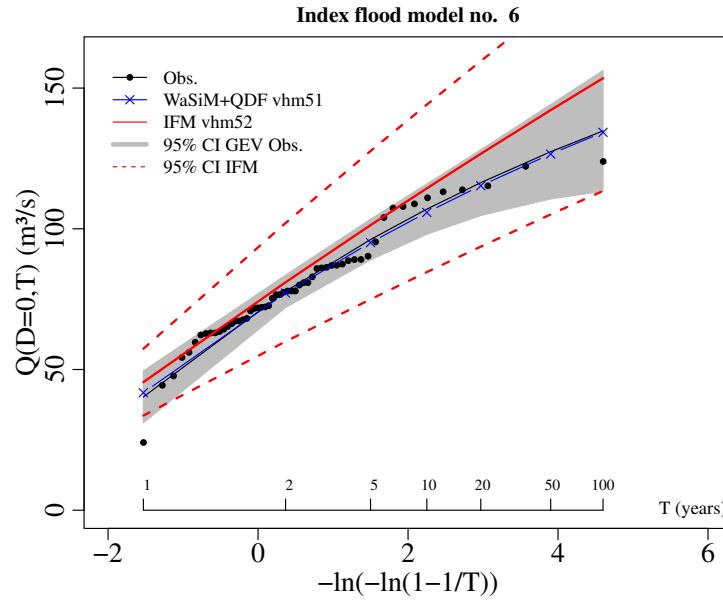


Figure 12. As Figure 11 but for Region 2. The solid blue and red lines correspond to results obtained with the index flood method developed with WaSiM simulations and QDF modeling within catchments vhm19 and vhm38, respectively.

Annual max. inst. Q : GEV Distributions for VHM51



Annual max. inst. Q : GEV Distributions for VHM52

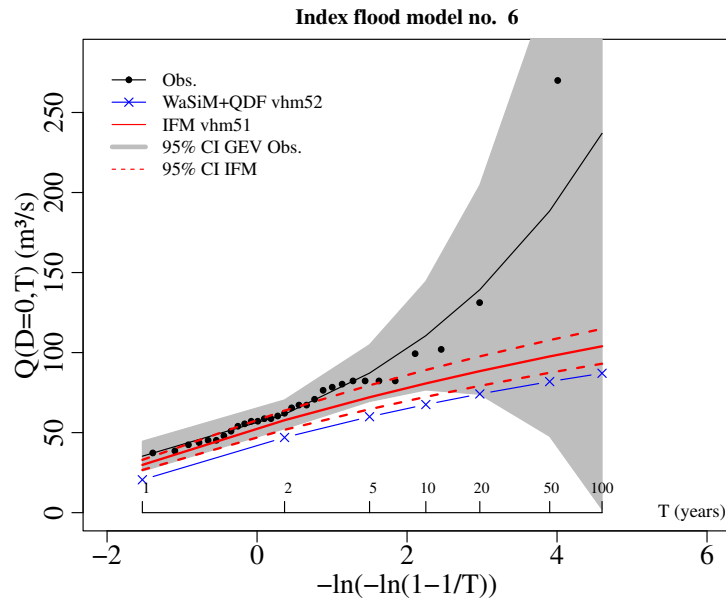
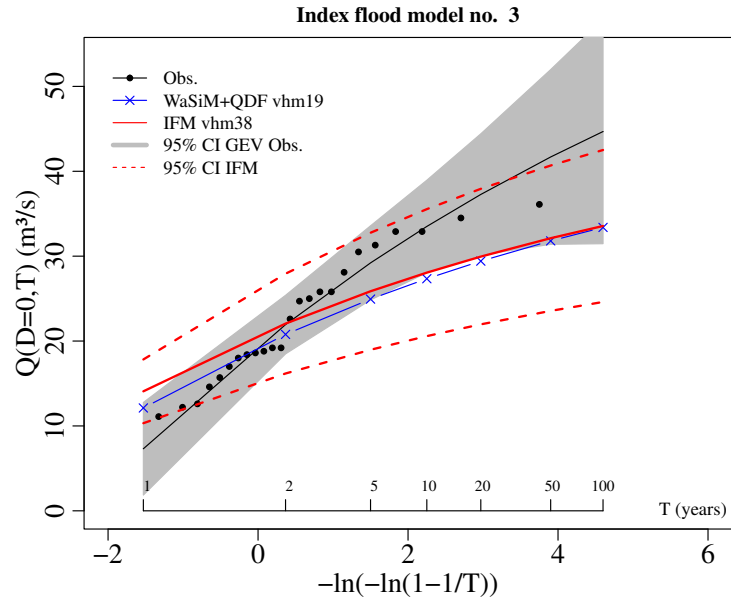


Figure 13. Region 1: Empirical and modeled instantaneous flood frequency distributions ($Q(D,T)$) at gauged sites vhm51 (top) and vhm52 (bottom). The solid black line corresponds to the reference GEV distribution derived from the observed AMF series. The solid blue line corresponds to the GEV distribution derived by QDF modeling of the simulated AMF series made with WaSiM at the gauged sites. The solid red line corresponds to the distribution estimated with the IFM (Eqs. 1 and 12) developed using WaSiM simulations and QDF modeling within vhm52 (top) and vhm51 (bottom). Dashed lines and shaded grey region correspond to the 95% confidence intervals (CI) (see Crochet 2012a). Uncertainties related to hydrological modeling and QDF modeling are not included in the CI calculation (CI IFM in figures legend).

Annual max. inst. Q : GEV Distributions for VHM19



Annual max. inst. Q : GEV Distributions for VHM38

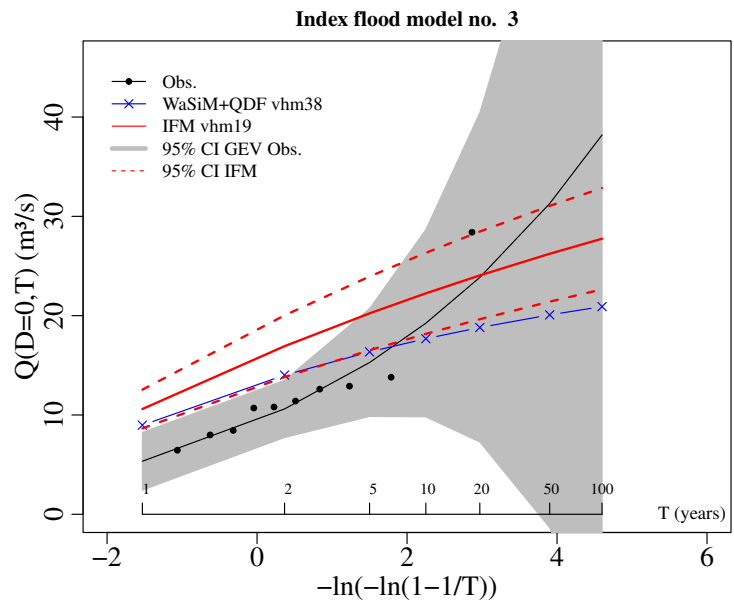


Figure 14. As for Fig. 13 but for catchments vhm19 (top) and vhm38 (bottom), located in Region 2. The solid red line corresponds to the distribution estimated with the IFM (Eqs. 1 and 9) developed using WaSiM simulations and QDF modeling within vhm38 (top) and vhm19 (bottom)

5 Conclusion and future research

Limited data availability is the most important difficulty that hydrologists and engineers face in the design of hydraulic structures. Regional flood frequency analysis offers a solution to this problem by pooling flood data from different gauged sites belonging to a homogeneous region, in order to predict flood quantiles at sites where streamflow series are short or at ungauged locations. However, the development of a robust method is challenging in regions where the number of gauged sites is limited.

The combined use of distributed hydrological modeling, QDF modeling and regional flood frequency analysis proposed in this study attempts to provide an answer to this problem. The distributed hydrological model WaSiM-ETH was calibrated on gauged catchments and used to simulate streamflow series at different locations within these catchments. Flood statistics were then extracted at these locations and used to develop a regional flood frequency analysis which was used to infer daily and instantaneous flood quantiles at totally ungauged catchments. The proposed method proved to offer a promising solution for estimating flood quantiles in regions where the limited number of gauged sites could limit or even prevent the development of the index flood method from streamflow observations. In principle, this method could be developed for an entire region even if one site only was gauged, as demonstrated in this study.

Whether the index flood method is developed with observed or simulated series, the main difficulty remains the same. It is difficult to estimate the index flood for catchments whose characteristics are far outside the range of characteristics used to develop the index flood regression models. In such a case, the model is extrapolated far beyond the range for which it was developed and the estimation is uncertain. An important under- or over-estimation of the catchment index flood will have a strong impact on the predicted flood quantiles, even if the regional growth curve is representative for the catchment of interest.

The combined methodology proposed in this study needs to be assessed in other regions and also developed further in the two studied regions, by including streamflow simulations from other gauged catchments. A study of the advantages and limitations of this method compared to the development of an index flood method based only on observations from available gauged sites needs to be conducted, as well as the possibility to combine simulations and observations.

Finally, an important aspect that remains to be investigated is the assessment of the uncertainties associated to the hydrological modeling and the QDF modeling and their inclusion in the calculation of the flood quantile uncertainty.

6 Acknowledgements

This study was supported by Vegagerðin (the Icelandic Road and Coastal Administration). The authors gratefully acknowledge Auður Atladóttir for her contribution to this study.

7 References

- Atladóttir, A., Crochet, P., Jónsson, S. & Hróðmarsson, H.B. (2011). Mat á flóðagreiningu með rennslisröðum reiknuðum með vatnafræðilíkaninu WaSiM. Frumniðurstöður fyrir vatnasvið á sunnanverðum Vestfjörðum. Icelandic Meteorological Office Rep. 2011-008, 41 pp.
- Bocchiola, D., De Michele, C. & Rosso, R. (2003). Review of recent advances in index flood estimation. *Hydrol. Earth Sys. Sci.*, 7(3), 283–296.
- Blazkova, S. & Beven, K. (1997). Flood frequency prediction for data limited catchments in the Czech Republic using a stochastic rainfall model and TOPMODEL. *J. Hydrol.*, 195, 256–278.
- Boughton, W. & Droop, O. (2003). Continuous simulation for design flood estimation – a review. *Environ. Model. Software*, 18, 309–318.
- Brath, A., Castellarin, A., Franchini, M. & Galeati, G. (2001). Estimating the index flood using indirect methods. *Hydrol. Sci. J.*, 46(3), 399–418.
- Burn, D.H. (1990). Evaluation of regional flood frequency analysis with a region of influence approach. *Water Resour. Res.*, 26(10), 2257–2265.
- Cameron, D.S., Beven, K.J., Tawn, J., Blazkova, S. & Naden, P. (1999). Flood frequency estimation by continuous simulation for a gauged upland catchment (with uncertainty). *J. Hydrol.*, 219, 169–187.
- Crochet, P. (2012a). Estimating the flood frequency distribution for ungauged catchments using an index flood procedure. Application to ten catchments in Northern Iceland. Icelandic Met. Office report No. VÍ 2012-005, 59pp.
- Crochet, P. (2012b). Evaluation of two delineation methods for regional flood frequency analysis in northern Iceland. Icelandic Met. Office report No. VÍ 2012-013, 55pp.
- Crochet, P. (2012c). Flood-duration-frequency modeling. Application to ten catchments in Northern Iceland. Icelandic Met. Office report No. VÍ 2012-006, 50pp.
- Crochet, P. (2012d). A semi-automatic multi-objective calibration of the WaSiM hydrological model. Icelandic Met. Office report No. PC/2012-01. 26pp.
- Crochet, P. (2013). Sensitivity of Icelandic river basins to recent climate variations. *Jökull*, 63, 71–90.
- Crochet, P. & Jóhannesson, T. (2011). A dataset of daily temperature in Iceland for the period 1949–2010. *Jökull*, 61, 1–17.
- Crochet, P., Jóhannesson, T., Jónsson, T., Sigurðsson, O., Björnsson, H., Pálsson, F. & Barstad, I. (2007). Estimating the spatial distribution of precipitation in Iceland using a linear model of orographic precipitation. *J. Hydrometeorol.*, 8, 1285–1306.
- Dalrymple, T. (1960). Flood frequency analysis. US Geol. Surv. Water Supply Paper, 1543 A.

- Das, S. & Cunnane, C. (2011). Examination of homogeneity of selected Irish pooling groups. *Hydrol. Earth Sys. Sci.*, 15, 819–830.
- Fiorentino, M., Manfreda, S. & Iacobellis, V. (2007). Peak runoff contributing area as hydrological signature of the probability distribution of floods. *Adv. Water Resour.*, 30, 2123–2134.
- Grell, G.L., Dudhia, J. & Stauffer, D.R. (1995). A description of the fifth-generation Penn State/NCAR Mesoscale Model (MM5). NCAR Tech. Note NCAR/TN-398+STR, 122p.
- GREHYS. (1996a). Presentation and review of some methods for regional flood frequency analysis. *J. Hydrol.*, 186, 63–84.
- GREHYS. (1996b). Inter-comparison of regional flood frequency procedures for Canadian rivers. *J. Hydrol.*, 186, 85–103.
- Grover, P.L., Burn, D.H. & Cunderlik, J.M. (2002). A comparison of index flood estimation procedures for ungauged catchments. *Can. J. Civ. Eng.*, 29, 731–741.
- Hoskings, J.R.M. & Wallis, J.R. (1993). Some statistics useful in regional frequency analysis. *Water. Resour. Res.* 29, 271-281.
- Hosking, J.R.M. & Wallis, J.R. (1997). *Regional frequency analysis. An approach based on L-Moments.* Cambridge University Press. 224pp.
- Hosking, J.R.M., Wallis, J.R. & Wood, E.F. (1985a). Estimation of the generalized extreme-value distribution by the method of the probability-weighted moments. *Technometrics*, 27(3), 251–261.
- Hosking, J.R.M., Wallis, J.R. & Wood, E.F. (1985b). An appraisal of the regional flood frequency procedure in the UK Flood Studies Report. *Hydrol. Sci. J.*, 30, 85–109.
- Javelle, P., Ouarda, T.B.M.J. & Bobée, B. (2003). Spring flood analysis using the flood-duration-frequency approach: Application to the provinces of Quebec and Ontario, Canada. *Hydrol. Proc.*, 17, 3717–3736.
- Jenkinson, A.F. (1955). The frequency distribution of the annual maximum (or minimum) of meteorological elements. *Quart. J. R. Met. Soc.* 81, 158–171.
- Jingyi, Z. & Hall, M.J. (2004). Regional flood frequency analysis for Gan-Ming river basin in China. *J. Hydrol.*, 296, 98–117.
- Kjeldsen, T.R. & Jones, D. (2007). Estimation of an index flood using data transfer in the UK. *Hydrol. Sci. J.*, 52(1), 86–98.
- Malekinezhad, H., Nachtnebel, H.P. & Klik, A. (2011a). Comparing the index flood and multiple-regression methods using L-moments. *J. Phys. Chem. Earth*, 36, 54–60.
- Malekinezhad, H., Nachtnebel, H.P. & Klik, A. (2011b). Regionalization approach for extreme flood analysis using L-moments. *J. Agr. Sci. Tech.*, 13, 1183–1196.
- Post, D.A. (2009). Regionalizing rainfall-runoff model parameters to predict the daily stream-flow of ungauged catchments in the dry tropics. *Hydrol. Res.*, 40.5, 433–444.

- Saliha, A.H., Awulachew, S.B., Cullmann, J. & Horlacher, H.B. (2011). Estimation of flow in ungauged catchments by coupling a hydrological model and neural networks: Case study. *Hydrol. Res.*, 42.5, 386–400.
- Schulla, J. & Jasper, K. (2007). Model Description WaSiM-ETH. Technical report, ETH Zürich, 181 pp.
- Stedinger, J.R., Vogel, R.M. & Foufoula-Georgiou, E. (1992). Frequency analysis of extreme events. *Handbook of Hydrology*, D.R. Maidment Ed., McGraw-Hill.
- Þórarinsdóttir, T. (2012). Development of a methodology for estimation of technical hydropower potential in Iceland using high resolution hydrological modeling. University of Iceland. 106pp.
- Zaman, M.A., Rahman, A. & Haddad, K. (2012). Regional flood frequency analysis in arid regions. A case study for Australia. *J. Hydrol.*, 475, 74-83.

Appendix I - Daily Index flood models for Region 1.

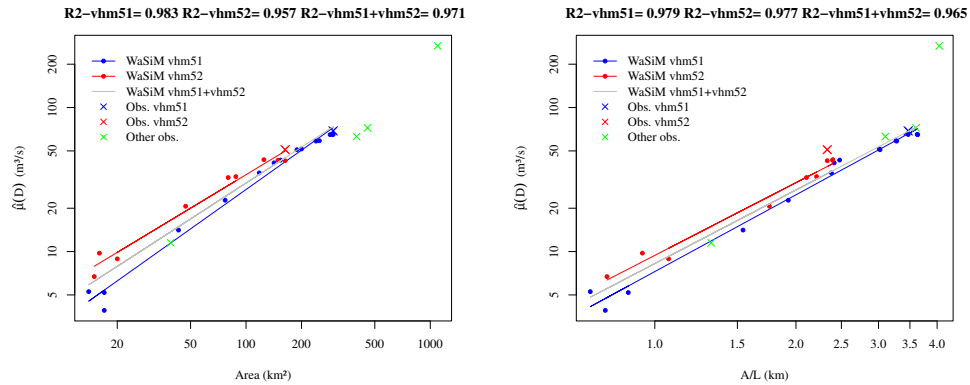


Figure I.1. Left-panel: $\mu(D)$ versus A (Eq. 7), right-panel: $\mu(D)$ versus A/L (Eq. 8).

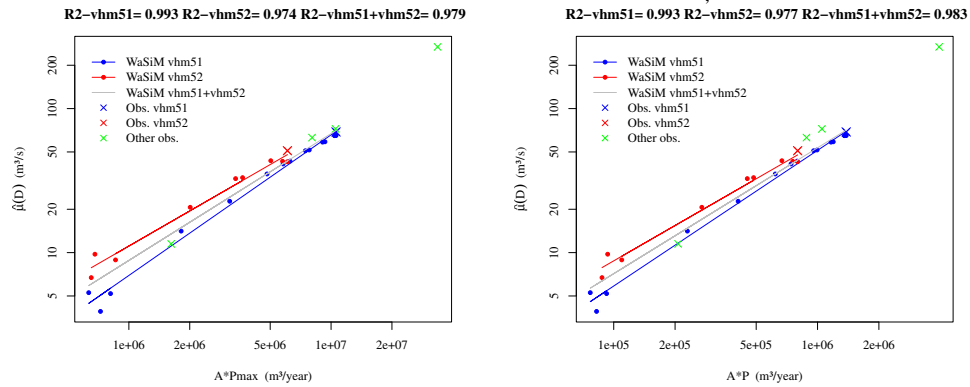


Figure I.2. Left-panel: $\mu(D)$ versus AP_m (Eq. 9), right-panel: $\mu(D)$ versus AP (Eq. 10).

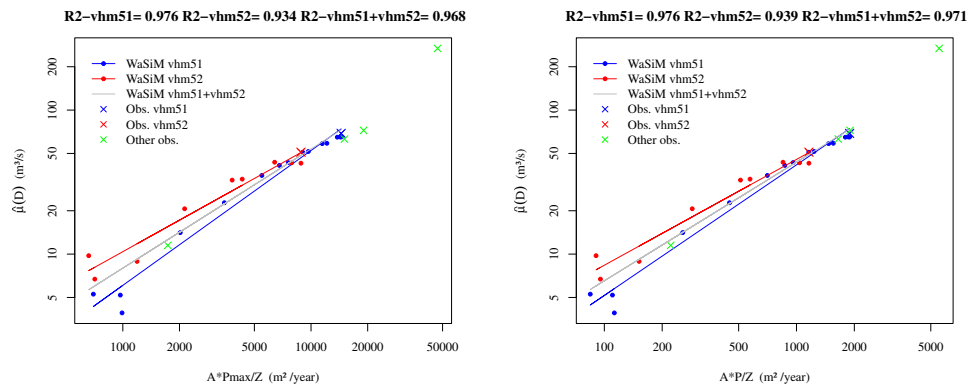


Figure I.3. Left-panel: $\mu(D)$ versus AP_m/Z (Eq. 11), right-panel: $\mu(D)$ versus AP/Z (Eq. 12).

Figure I: Calibration of the daily index flood models (Eqs. 7 to 12) by linear regression using WaSiM streamflow simulations within catchment vhm51 only (solid blue line), catchment vhm52 only (solid red line) and both catchments (solid grey line). The green symbols correspond to the observations made at the other gauged sites (vhm92, vhm10, vhm45 and vhm200).

Appendix II - Daily Index flood models for Region 2.

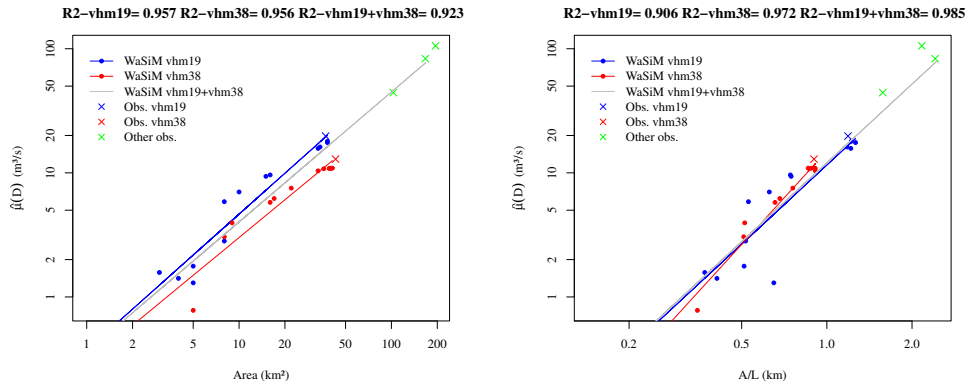


Figure II.1. Left-panel: $\mu(D)$ versus A (Eq. 7), right-panel: $\mu(D)$ versus A/L (Eq. 8).

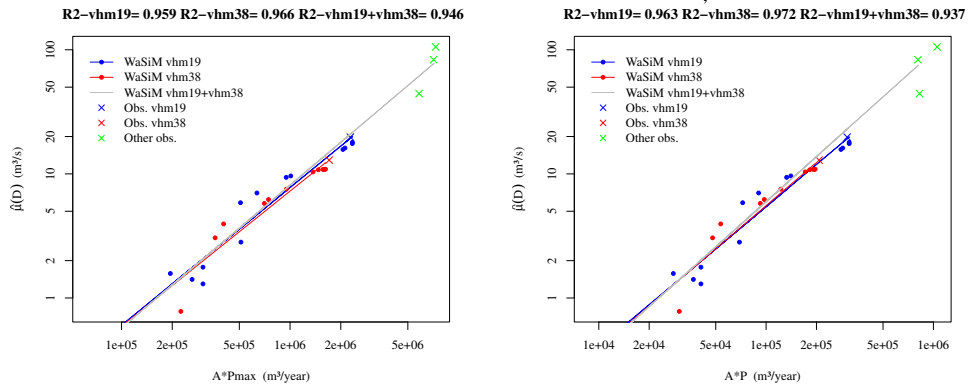


Figure II.2. Left-panel: $\mu(D)$ versus AP_m (Eq. 9), right-panel: $\mu(D)$ versus AP (Eq. 10).

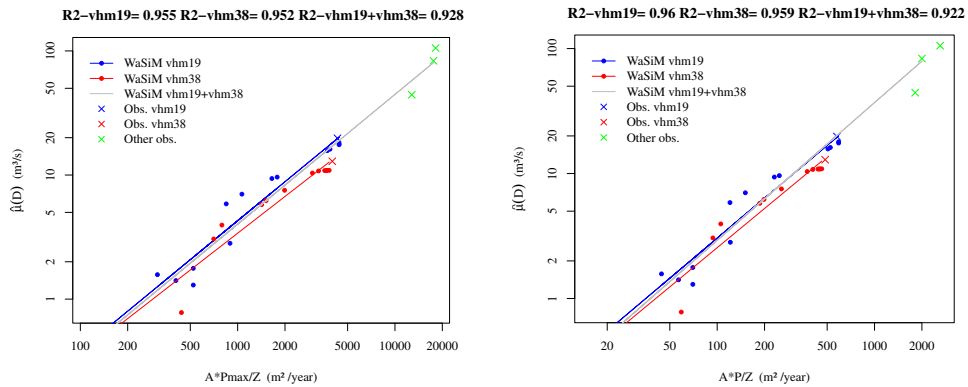


Figure II.3. Left-panel: $\mu(D)$ versus AP_m/Z (Eq. 11), right-panel: $\mu(D)$ versus AP/Z (Eq. 12).

Figure II: Calibration of the daily index flood models (Eqs. 7 to 12) by linear regression using WaSiM streamflow simulations within catchment vhm19 only (solid blue line), catchment vhm38 only (solid red line) and both catchments (solid grey line). The green symbols correspond to the observations made at the other gauged sites (vhm12, vhm204 and vhm198).

Appendix III - Comparison between reference and estimated daily index floods for Region 1.

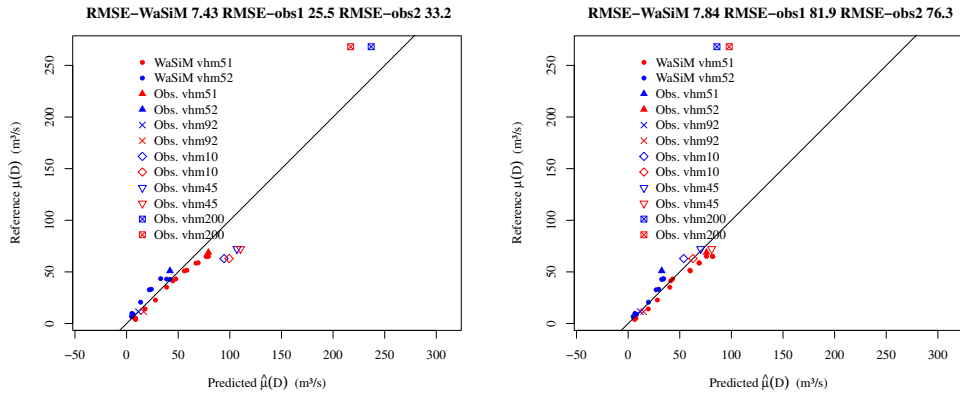


Figure III.1. Left-panel: $\hat{\mu}(D) = a(A)^b$ (Eq. 7), right-panel: $\hat{\mu}(D) = a(A/L)^b$ (Eq. 8).

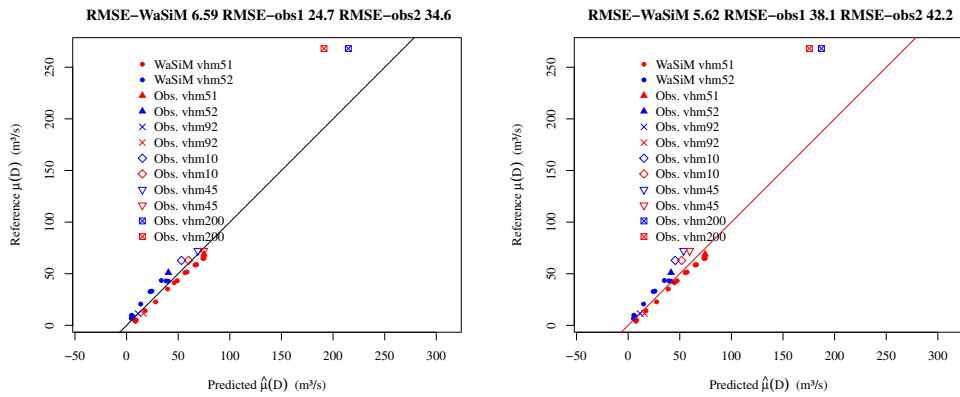


Figure III.2. Left-panel: $\hat{\mu}(D) = a(AP_m)^b$ (Eq. 9), right-panel: $\hat{\mu}(D) = a(AP)^b$ (Eq. 10).

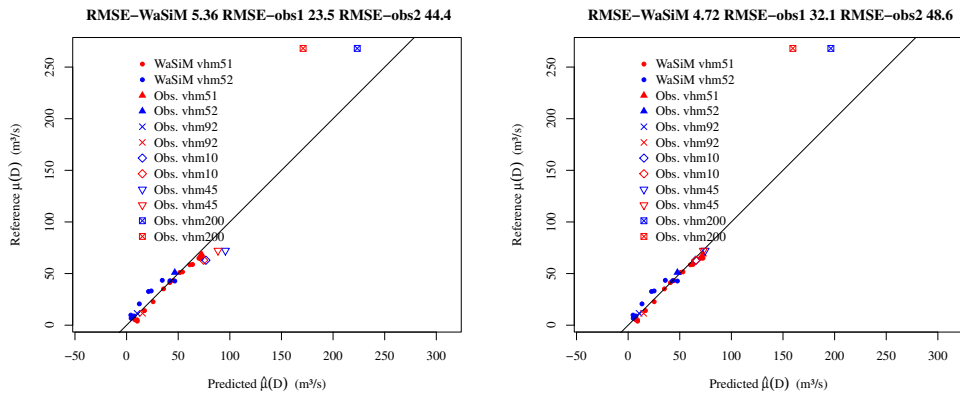


Figure III.3. Left-panel: $\hat{\mu}(D) = a(AP_m/Z)^b$ (Eq. 11), right-panel: $\hat{\mu}(D) = a(AP/Z)^b$ (Eq. 12).

Figure III: Comparison between reference ($\mu(D)$) and estimated ($\hat{\mu}(D)$) daily index floods at gauged and simulated sites, using index flood models developed with WaSiM simulations within catchment vhm51 (blue) and catchment vhm52 (red). The reference is the mean of the observed AMF series at gauged sites and the mean of the simulated AMF series made with WaSiM within catchments vhm52 and then vhm51. The solid line represents the 1:1 line.

Appendix IV - Comparison between reference and estimated daily index floods for Region 2.

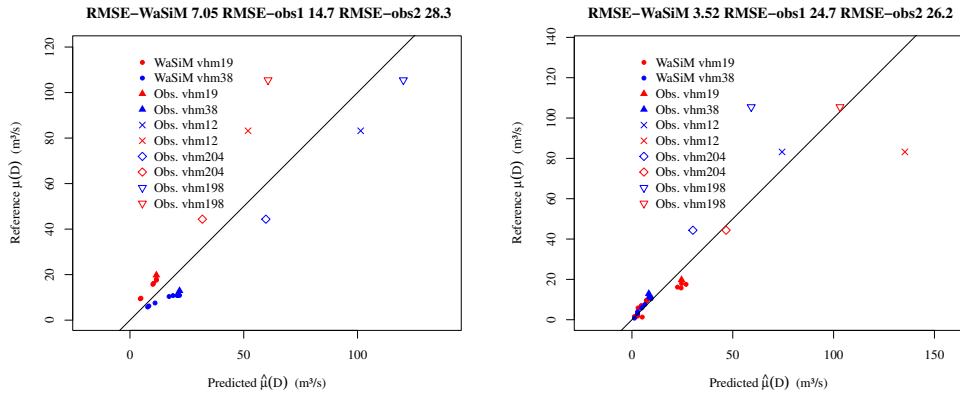


Figure IV.1. Left-panel: $\hat{\mu}(D) = a(A)^b$ (Eq. 7), right-panel: $\hat{\mu}(D) = a(A/L)^b$ (Eq. 8).

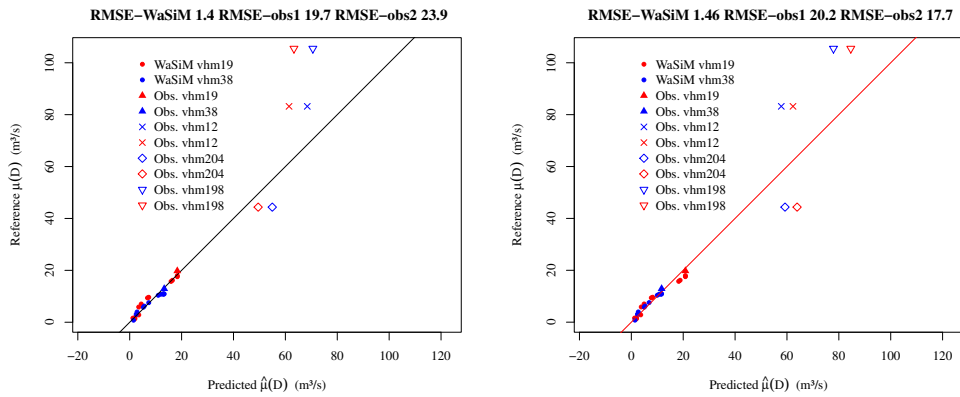


Figure IV.2. Left-panel: $\hat{\mu}(D) = a(AP_m)^b$ (Eq. 9), right-panel: $\hat{\mu}(D) = a(AP)^b$ (Eq. 10).

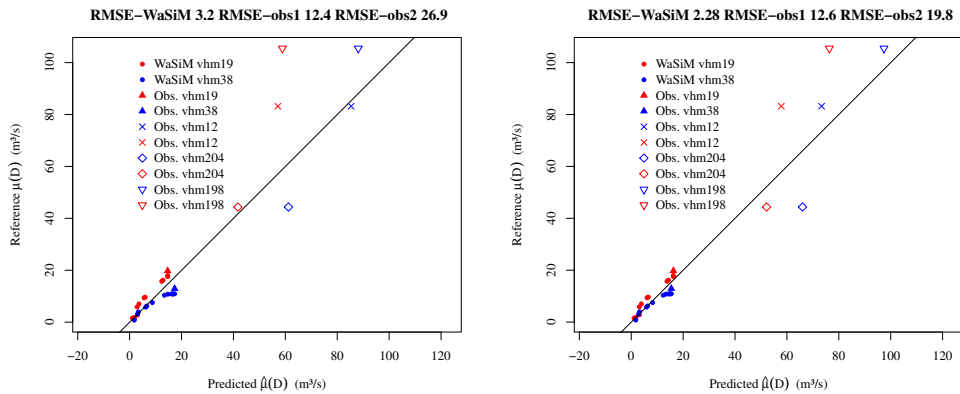


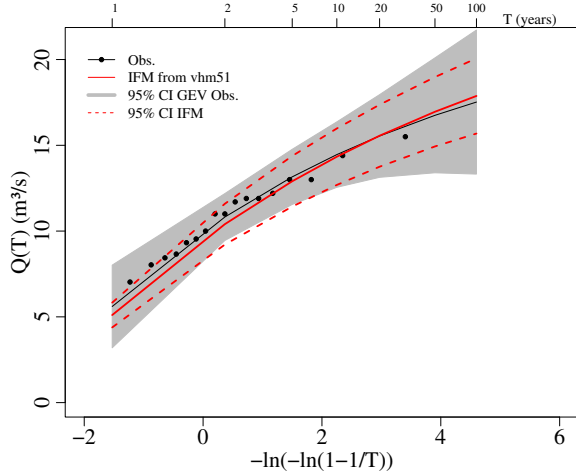
Figure IV.3. Left-panel: $\hat{\mu}(D) = a(AP_m/Z)^b$ (Eq. 11), right-panel: $\hat{\mu}(D) = a(AP/Z)^b$ (Eq. 12).

Figure IV: Comparison between reference ($\mu(D)$) and estimated ($\hat{\mu}(D)$) daily index floods at gauged and simulated sites, using index flood models developed with WaSiM simulations within catchment vhm19 (blue) and catchment vhm38 (red). The reference is the mean of the observed AMF series at gauged sites and the mean of the simulated AMF series made with WaSiM within catchments vhm38 and then vhm19. The solid line represents the 1:1 line.

Appendix V - Empirical and modeled daily flood frequency distributions for Region 1 derived with index flood model no. 6:

$$\hat{\mu}(D) = a(AP/Z)^b$$

Annual max. Q : GEV Distributions for vhm 92 using IFM developed with vhm51
Index flood model no. 6



Annual max. Q : GEV Distributions for vhm 92 using IFM developed with vhm52
Index flood model no. 6

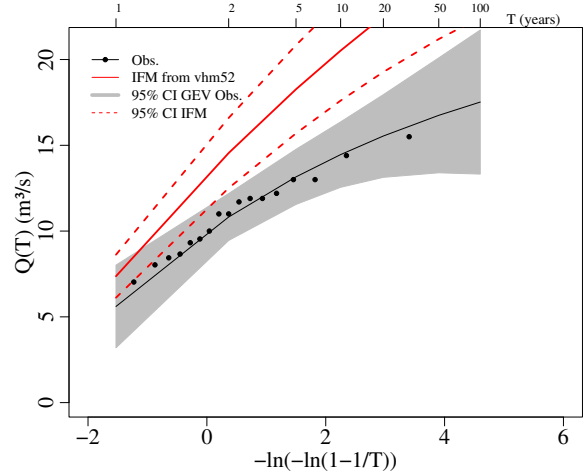
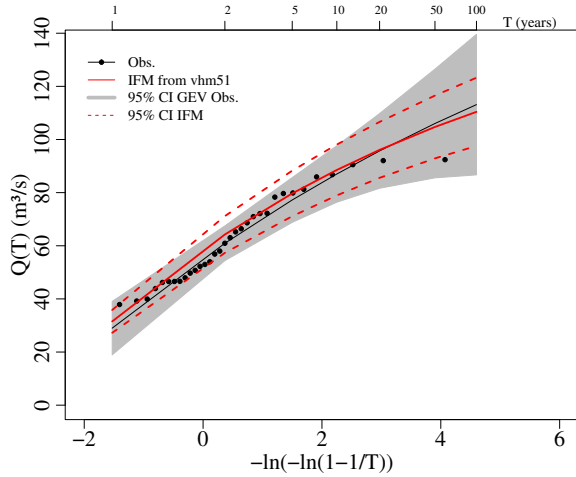


Figure V.1. Estimation at vhm92 with the IFM developed within vhm51 (left) and within vhm52 (right).

Annual max. Q : GEV Distributions for vhm 10 using IFM developed with vhm51
Index flood model no. 6



Annual max. Q : GEV Distributions for vhm 10 using IFM developed with vhm52
Index flood model no. 6

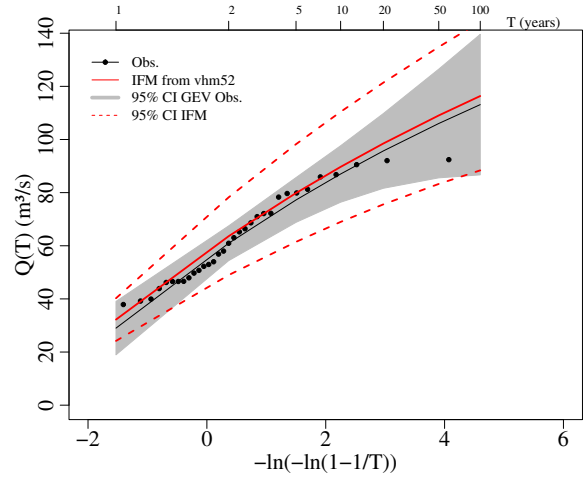
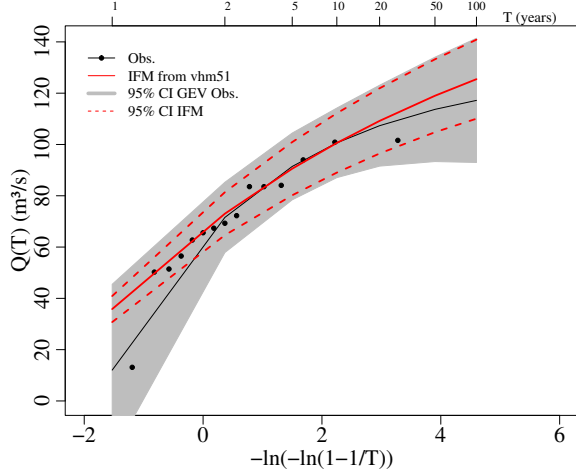


Figure V.2. Estimation at vhm10 with the IFM developed within vhm51 (left) and within vhm52 (right).

Figure V: Empirical and modeled daily flood frequency distributions ($Q(D,T)$) for Region 1. Black solid line: reference GEV distribution derived from the observed AMF series. Solid red line: GEV distribution estimated with the IFM ($\hat{Q}_i(D,T) = \hat{\mu}_i(D)q_R(D,T)$ with $\hat{\mu}_i(D) = a(A_iP_i/Z_i)^b$) developed using WaSiM simulations within vhm51 (left) and vhm52 (right). Dashed lines and shaded grey region correspond to the 95% confidence intervals (CI) (see Crochet 2012a). Uncertainty related to hydrological modeling is not included in the CI calculation (CI IFM in figures legend).

Annual max. Q : GEV Distributions for vhm 45 using IFM developed with vhm51
Index flood model no. 6



Annual max. Q : GEV Distributions for vhm 45 using IFM developed with vhm52
Index flood model no. 6

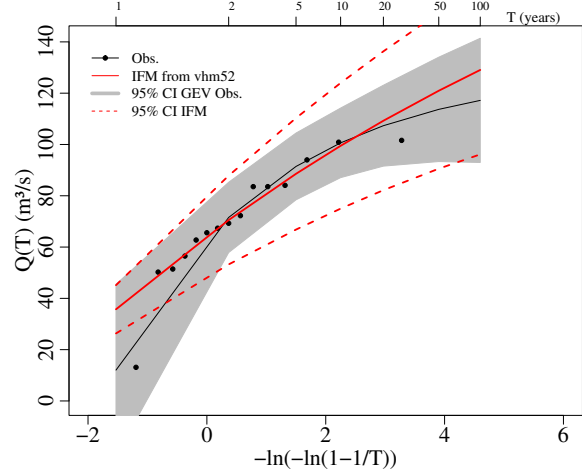
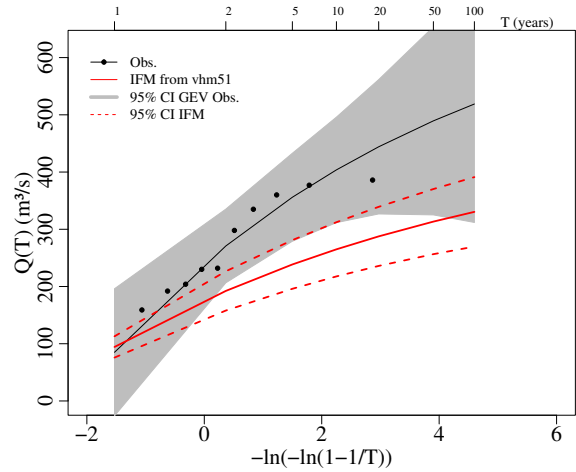


Figure V.3. Estimation at vhm45 with the IFM developed within vhm51 (left) and within vhm52 (right).

Annual max. Q : GEV Distributions for vhm 200 using IFM developed with vhm51
Index flood model no. 6



Annual max. Q : GEV Distributions for vhm 200 using IFM developed with vhm52
Index flood model no. 6

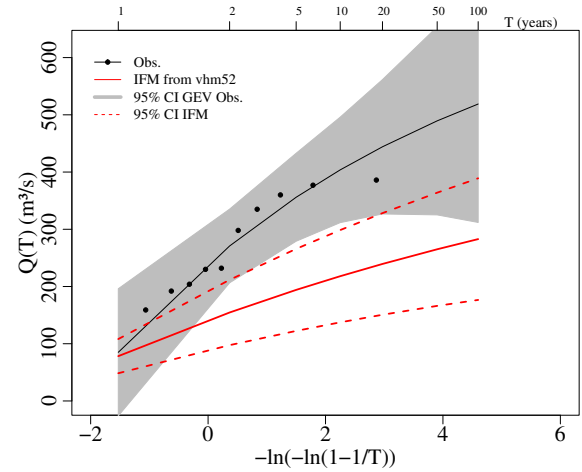


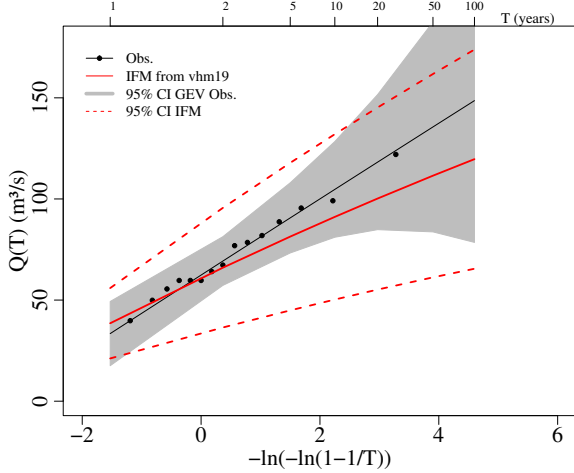
Figure V.4. Estimation at vhm200 with the IFM developed within vhm51 (left) and within vhm52 (right).

Figure V: Empirical and modeled daily flood frequency distributions ($Q(D,T)$) for Region 1. Black solid line: reference GEV distribution derived from the observed AMF series. Solid red line: GEV distribution estimated with the IFM ($\hat{Q}_i(D,T) = \hat{\mu}_i(D)q_R(D,T)$ with $\hat{\mu}_i(D) = a(A_iP_i/Z_i)^b$) developed using WaSiM simulations within vhm51 (left) and vhm52 (right). Dashed lines and shaded grey region correspond to the 95% confidence intervals (CI) (see Crochet 2012a). Uncertainty related to hydrological modeling is not included in the CI calculation (CI IFM in figures legend).

Appendix VI - Empirical and modeled daily flood frequency distributions for Region 2 derived with index flood model no. 3:

$$\hat{\mu}(D) = a(APm)^b$$

Annual max. Q : GEV Distributions for vhm 12 using IFM developed with vhm19
Index flood model no. 3



Annual max. Q : GEV Distributions for vhm 12 using IFM developed with vhm38
Index flood model no. 3

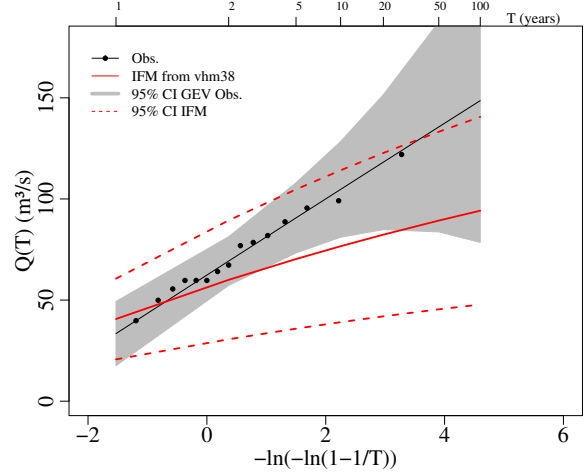
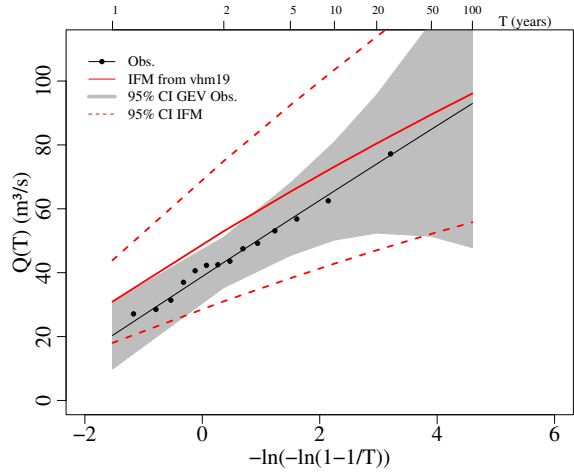


Figure VI.1. Estimation at vhm12 with the IFM developed within vhm19 (left) and within vhm38 (right).

Annual max. Q : GEV Distributions for vhm 204 using IFM developed with vhm19
Index flood model no. 3



Annual max. Q : GEV Distributions for vhm 204 using IFM developed with vhm38
Index flood model no. 3

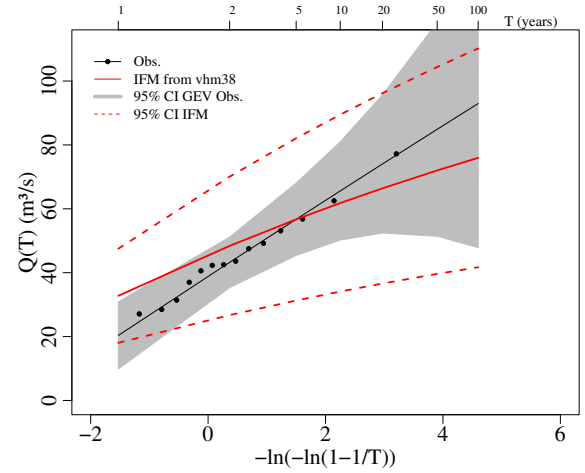
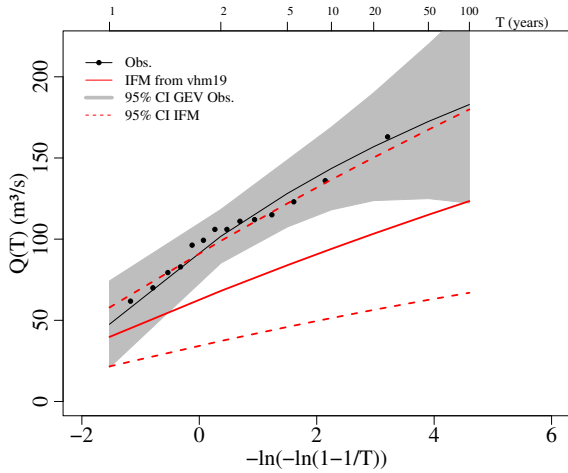


Figure VI.2. Estimation at vhm204 with the IFM developed within vhm19 (left) and within vhm38 (right).

Figure VI: Empirical and modeled daily flood frequency distributions ($Q(D,T)$) for Region 2. Black solid line: reference GEV distribution derived from the observed AMF series. Solid red line: GEV distribution estimated with the IFM ($\hat{Q}_i(D,T) = \hat{\mu}_i(D)q_R(D,T)$ with $\hat{\mu}_i(D) = a(A_i P m_i)^b$) developed using WaSiM simulations within vhm19 (left) and vhm38 (right). Dashed lines and shaded grey region correspond to the 95% confidence intervals (CI) (see Crochet 2012a). Uncertainty related to hydrological modeling is not included in the CI calculation (CI IFM in figures legend).

Annual max. Q : GEV Distributions for vhm 198 using IFM developed with vhm19
Index flood model no. 3



Annual max. Q : GEV Distributions for vhm 198 using IFM developed with vhm38
Index flood model no. 3

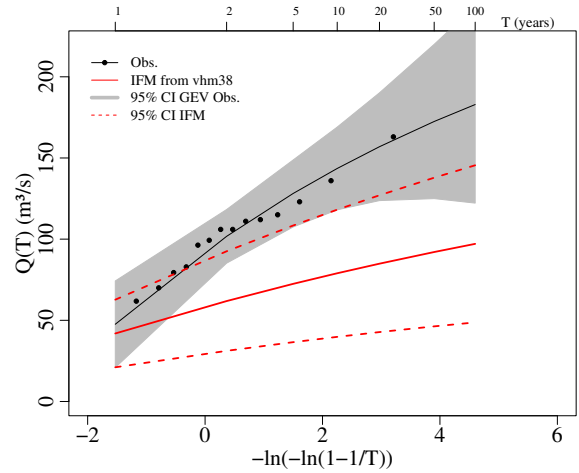


Figure VI.3. Estimation at vhm198 with the IFM developed within vhm19 (left) and within vhm38 (right).

Figure VI: Empirical and modeled daily flood frequency distributions ($Q(D,T)$) for Region 2. Black solid line: reference GEV distribution derived from the observed AMF series. Solid red line: GEV distribution estimated with the IFM ($\hat{Q}_i(D,T) = \hat{\mu}_i(D)q_R(D,T)$ with $\hat{\mu}_i(D) = a(A_i P m_i)^b$) developed using WaSiM simulations within vhm19 (left) and vhm38 (right). Dashed lines and shaded grey region correspond to the 95% confidence intervals (CI) (see Crochet 2012a). Uncertainty related to hydrological modeling is not included in the CI calculation (CI IFM in figures legend).

Appendix VII - Instantaneous Index flood models for Region 1.

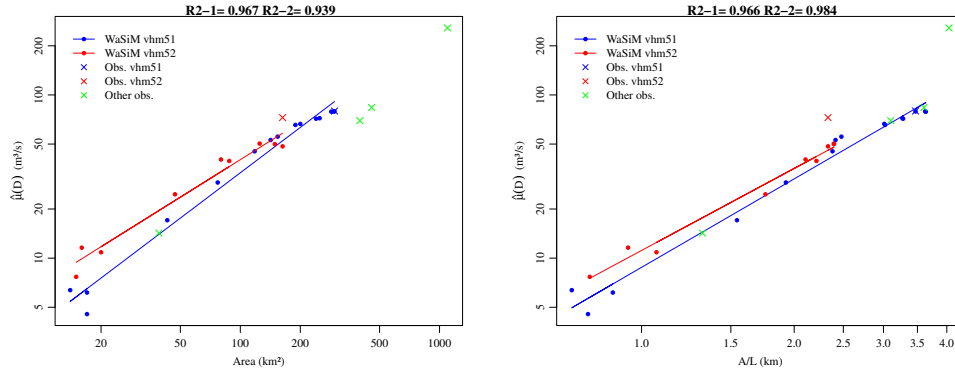


Figure VII.1. Left-panel: $\mu(D)$ versus A (Eq. 7), right-panel: $\mu(D)$ versus A/L (Eq. 8).

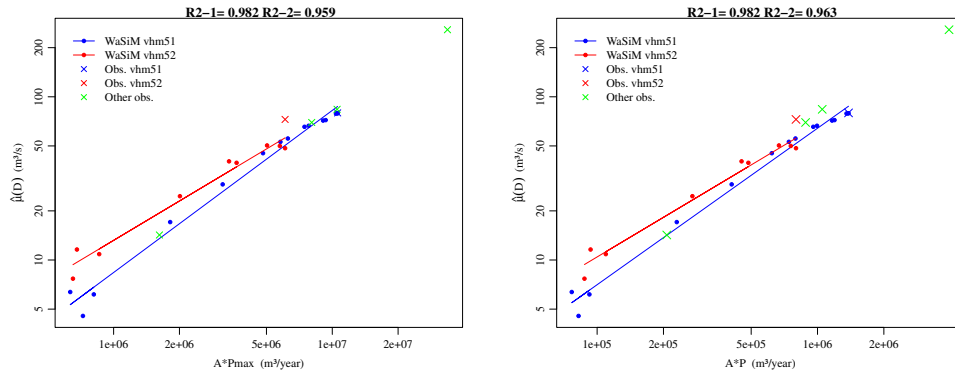


Figure VII.2. Left-panel: $\mu(D)$ versus AP_m (Eq. 9), right-panel: $\mu(D)$ versus AP (Eq. 10).

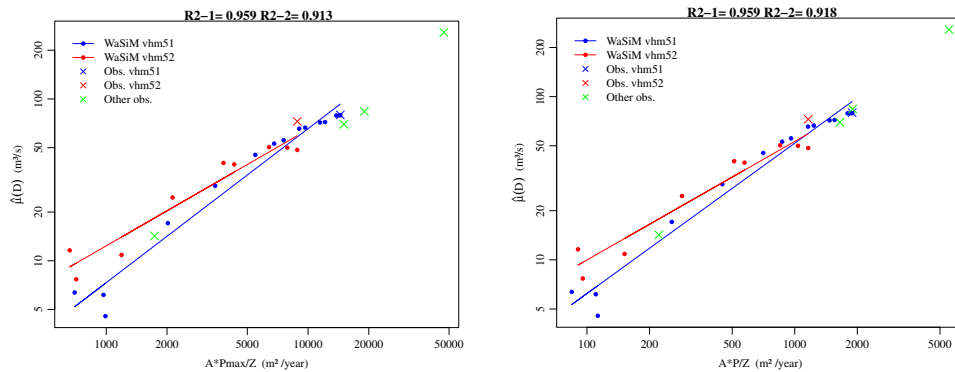


Figure VII.3. Left-panel: $\mu(D)$ versus AP_m/Z (Eq. 11), right-panel: $\mu(D)$ versus AP/Z (Eq. 12).

Figure VII: Calibration of the instantaneous index flood models (Eqs. 7 to 12) by linear regression using WaSiM streamflow simulations and QDF modeling within catchment vhm51 only (solid blue line) and catchment vhm52 only (solid red line). The green symbols correspond to the observations made at the other gauged sites (vhm92, vhm10, vhm45 and vhm200).

Appendix VIII - Instantaneous Index flood models for Region 2.

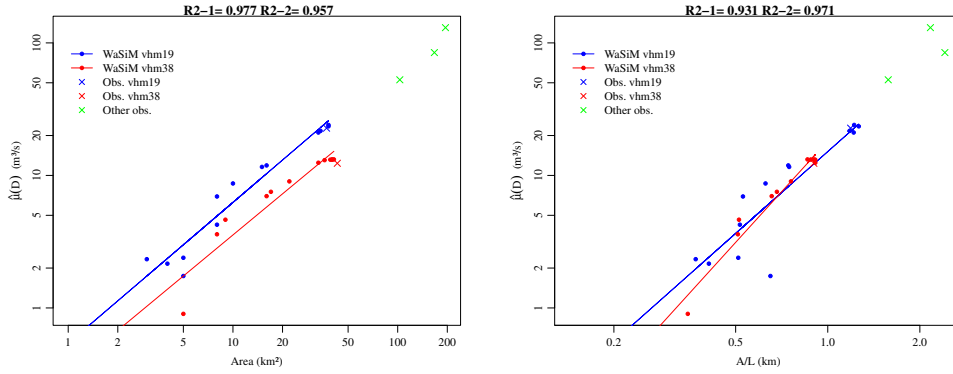


Figure VIII.1. Left-panel: $\mu(D)$ versus A (Eq. 7), right-panel: $\mu(D)$ versus A/L (Eq. 8).

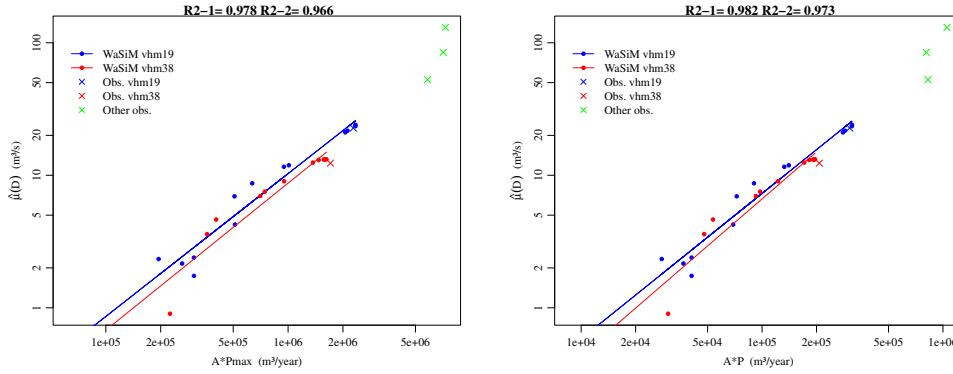


Figure VIII.2. Left-panel: $\mu(D)$ versus AP_m (Eq. 9), right-panel: $\mu(D)$ versus AP (Eq. 10).

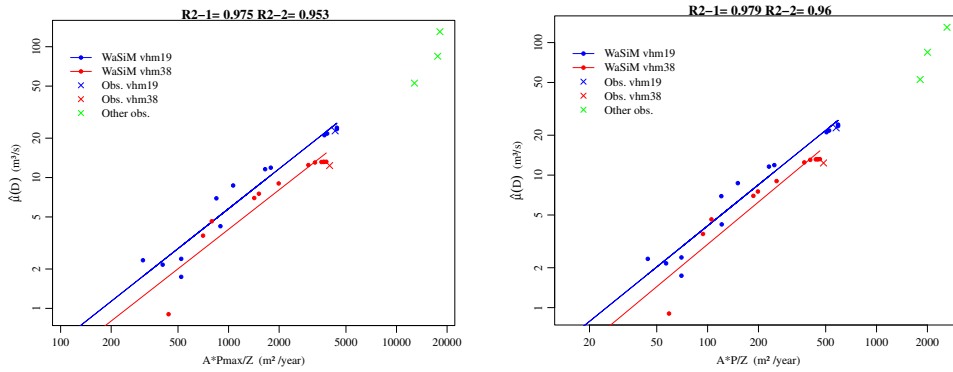


Figure VIII.3. Left-panel: $\mu(D)$ versus AP_m/Z (Eq. 11), right-panel: $\mu(D)$ versus AP/Z (Eq. 12).

Figure VIII: Calibration of the instantaneous index flood models (Eqs. 7 to 12) by linear regression using WaSiM streamflow simulations and QDF modeling within catchment vhm19 only (solid blue line) and catchment vhm38 only (solid red line). The green symbols correspond to the observations made at the other gauged sites (vhm12, vhm204 and vhm198).

Appendix IX - Comparison between reference and estimated instantaneous index floods for Region 1.

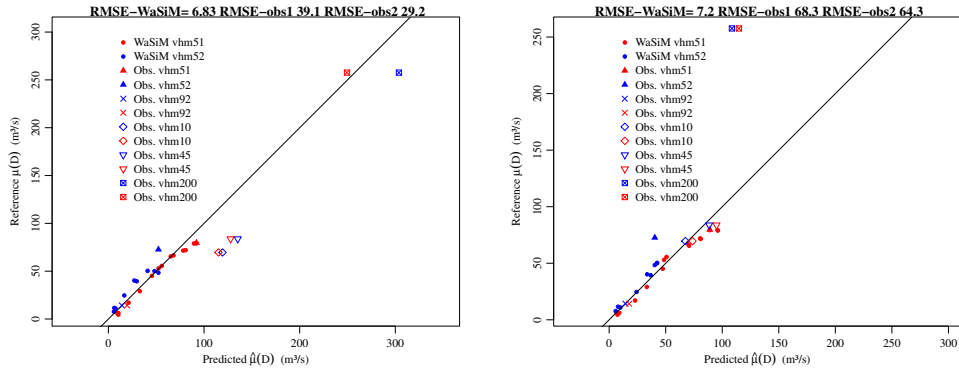


Figure IX.1. Left-panel: $\hat{\mu}(D) = a(A)^b$ (Eq. 7), right-panel: $\hat{\mu}(D) = a(A/L)^b$ (Eq. 8).

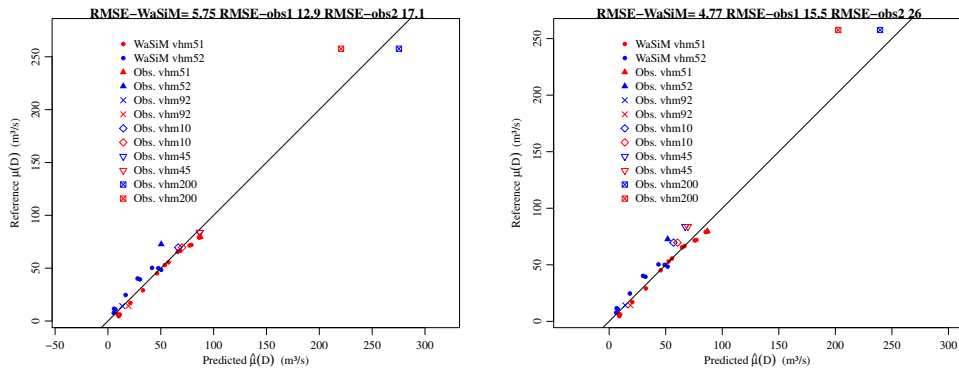


Figure IX.2. Left-panel: $\hat{\mu}(D) = a(AP_m)^b$ (Eq. 9), right-panel: $\hat{\mu}(D) = a(AP)^b$ (Eq. 10).

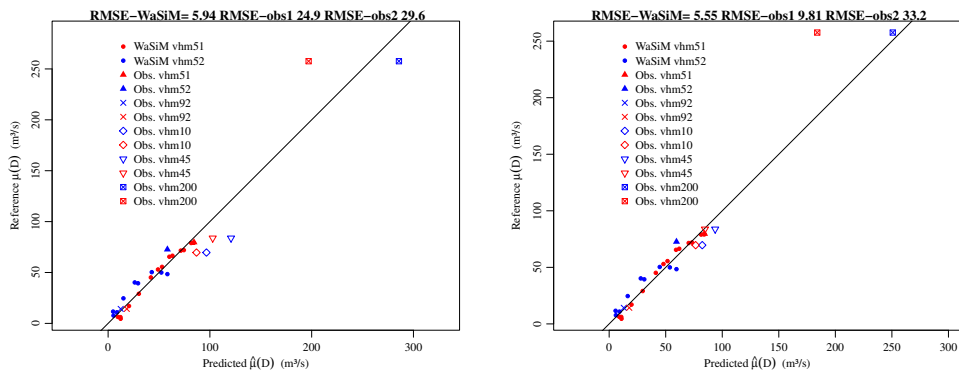


Figure IX.3. Left-panel: $\hat{\mu}(D) = a(AP_m/Z)^b$ (Eq. 11), right-panel: $\hat{\mu}(D) = a(AP/Z)^b$ (Eq. 12).

Figure IX: Comparison between reference ($\mu(D)$) and estimated ($\hat{\mu}(D)$) instantaneous index floods at gauged and simulated sites using index flood models developed with WaSiM simulations and QDF modeling within catchment vhm51 (blue) and catchment vhm52 (red). The reference is the mean of the observed AMF series at gauged sites and the index flood derived by QDF modeling of the simulated AMF series made with WaSiM within catchments vhm52 and then vhm51. The solid line represents the 1:1 line.

Appendix X - Comparison between reference and estimated instantaneous index floods for Region 2.

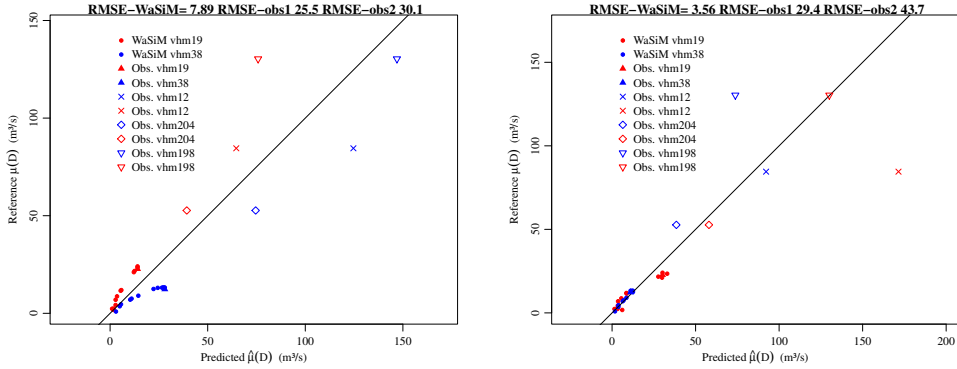


Figure X.1. Left-panel: $\hat{\mu}(D) = a(A)^b$ (Eq. 7), right-panel: $\hat{\mu}(D) = a(A/L)^b$ (Eq. 8).

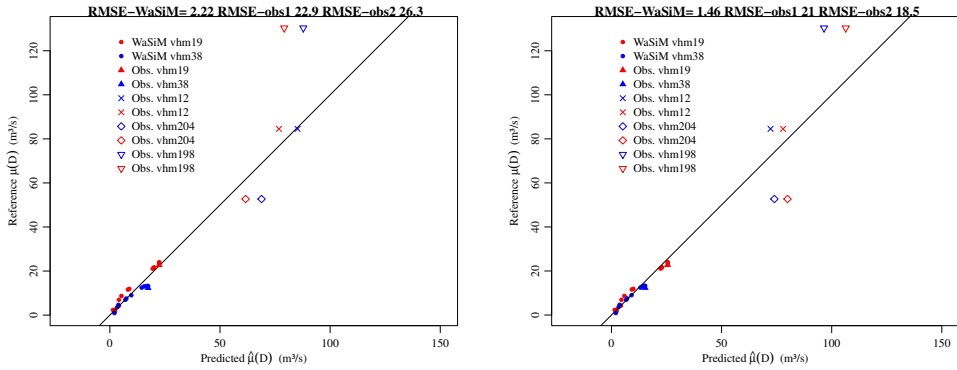


Figure X.2. Left-panel: $\hat{\mu}(D) = a(AP_m)^b$ (Eq. 9), right-panel: $\hat{\mu}(D) = a(AP)^b$ (Eq. 10).

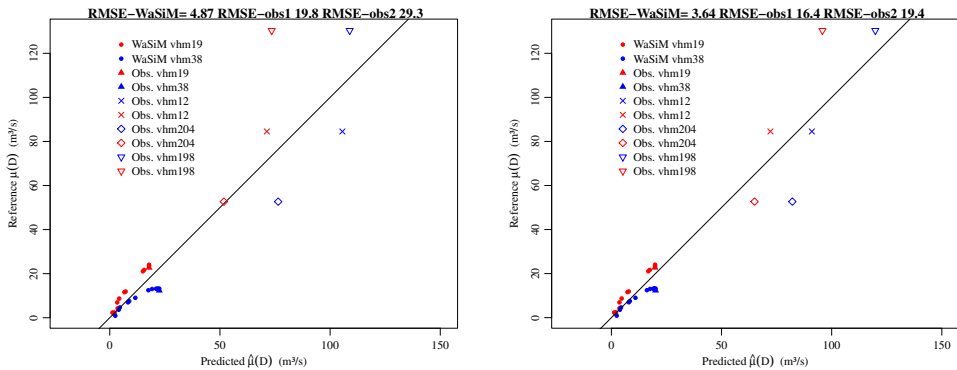


Figure X.3. Left-panel: $\hat{\mu}(D) = a(AP_m/Z)^b$ (Eq. 11), right-panel: $\hat{\mu}(D) = a(AP/Z)^b$ (Eq. 12).

Figure X: Comparison between reference ($\mu(D)$) and estimated ($\hat{\mu}(D)$) instantaneous index floods at gauged and simulated sites using index flood models developed with WaSiM simulations and QDF modeling within catchment vhm19 (blue) and catchment vhm38 (red). The reference is the mean of the observed AMF series at gauged sites and the index flood derived by QDF modeling of the simulated AMF series made with WaSiM within catchments vhm38 and then vhm19. The solid line represents the 1:1 line.

Appendix XI - Empirical and modeled instantaneous flood frequency distributions for Region 1 derived with index flood model no. 6: $\hat{\mu}(D) = a(AP/Z)^b$

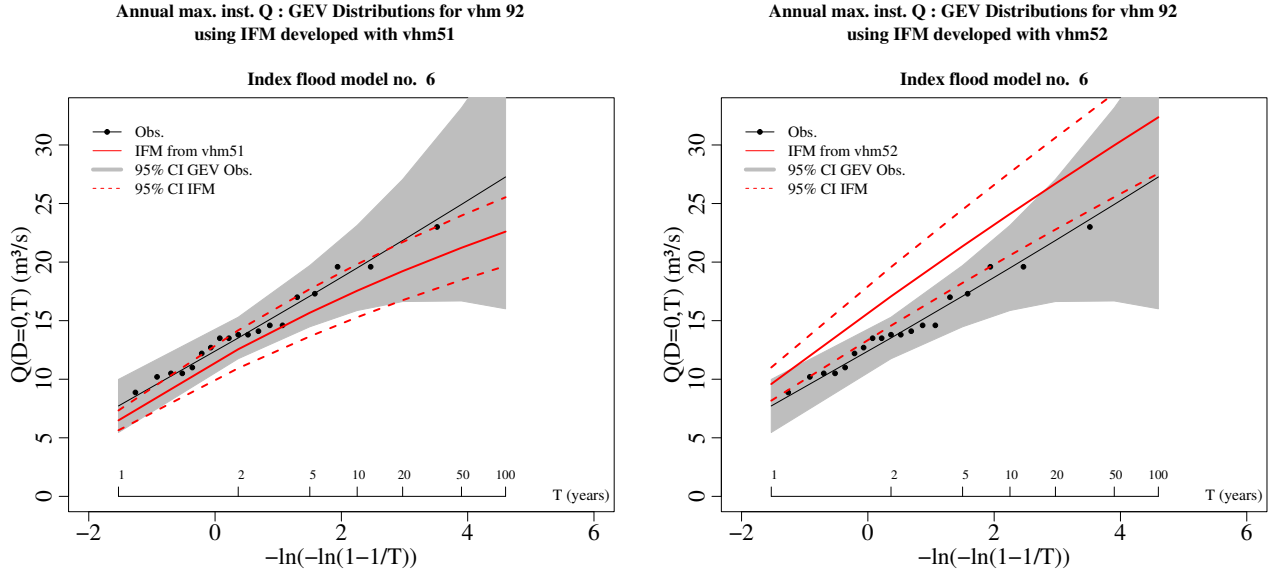


Figure XI.1. Estimation at vhm92 with the IFM developed within vhm51 (left) and within vhm52 (right).

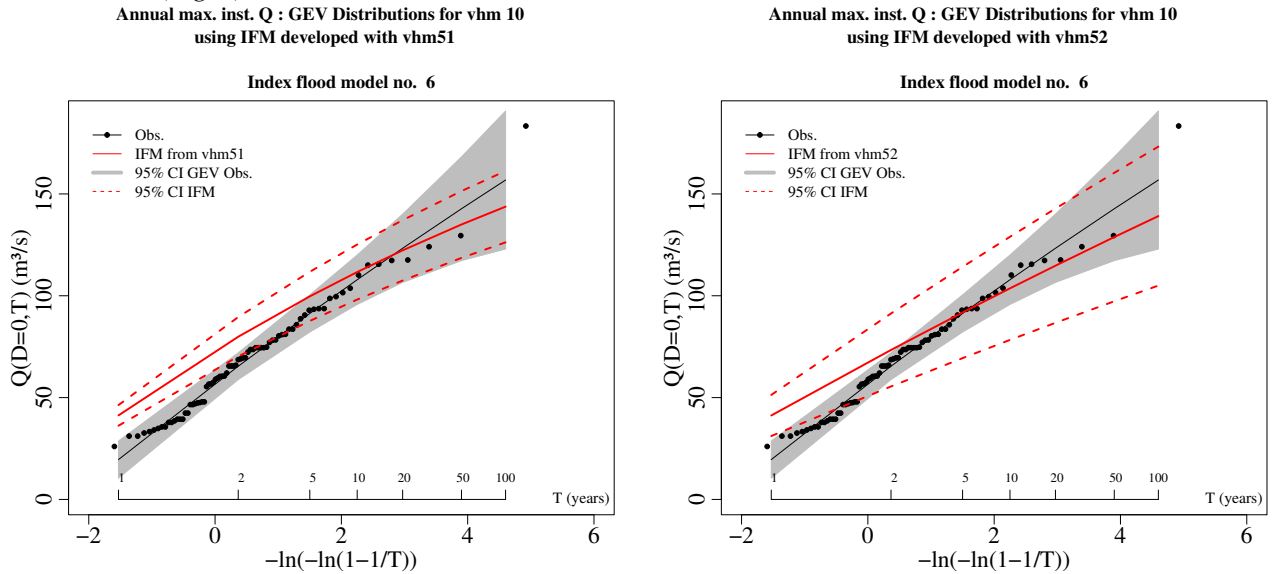


Figure XI.2. Estimation at vhm10 with the IFM developed within vhm51 (left) and within vhm52 (right).

Figure XI: Empirical and modeled instantaneous flood frequency distributions ($Q(D,T)$) for Region 1. Black solid line: reference GEV distribution derived from the observed AMF series. Solid red line: GEV distribution estimated with the IFM ($\hat{Q}_i(D,T) = \hat{\mu}_i(D)q_R(D,T)$ with $\hat{\mu}_i(D) = a(A_iP_i/Z_i)^b$) developed using WaSiM simulations and QDF modeling within vhm51 (left) and vhm52 (right). Dashed lines and shaded grey region correspond to the 95% confidence intervals (CI) (see Crochet 2012a). Uncertainties related to hydrological modeling and QDF modeling are not included in the CI calculation (CI IFM in figures legend).

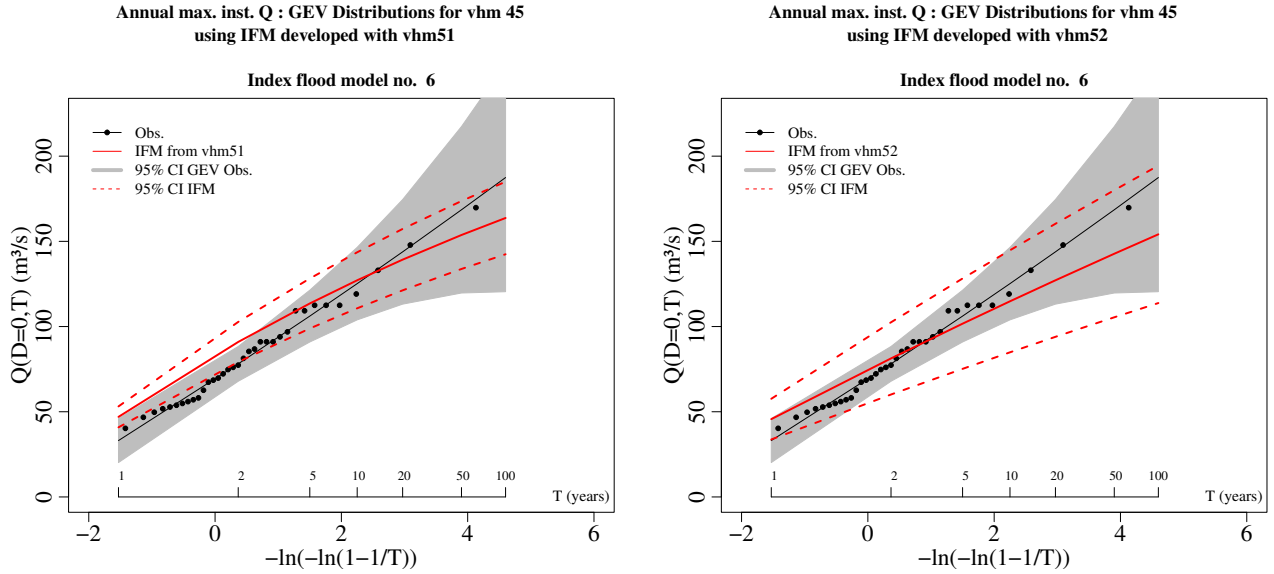


Figure XI.3. Estimation at vhm45 with the IFM developed within vhm51 (left) and within vhm52 (right).

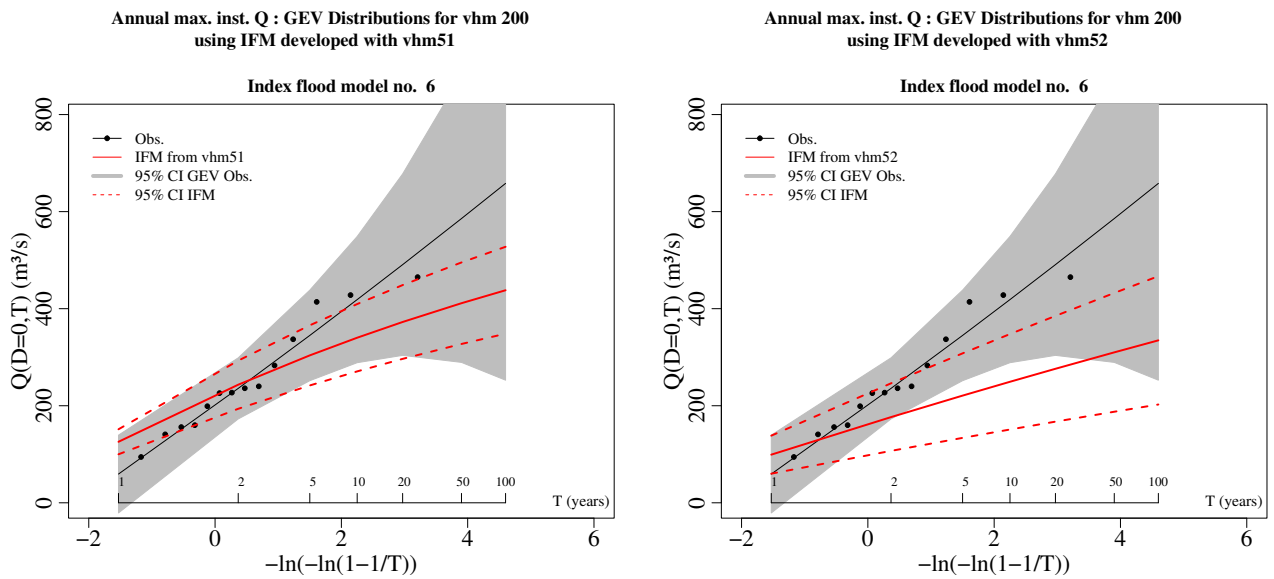


Figure XI.4. Estimation at vhm200 with the IFM developed within vhm51 (left) and within vhm52 (right).

Figure XI: Empirical and modeled instantaneous flood frequency distributions ($Q(D,T)$) for Region 1. Black solid line: reference GEV distribution derived from the observed AMF series. Solid red line: GEV distribution estimated with the IFM ($\hat{Q}_i(D,T) = \hat{\mu}_i(D)q_R(D,T)$ with $\hat{\mu}_i(D) = a(A_iP_i/Z_i)^b$) developed using WaSiM simulations and QDF modeling within vhm51 (left) and vhm52 (right). Dashed lines and shaded grey region correspond to the 95% confidence intervals (CI) (see Crochet 2012a). Uncertainties related to hydrological modeling and QDF modeling are not included in the CI calculation (CI IFM in figures legend).

Appendix XII - Empirical and modeled instantaneous flood frequency distributions for Region 2 derived with index flood model no. 3: $\hat{\mu}(D) = a(APm)^b$

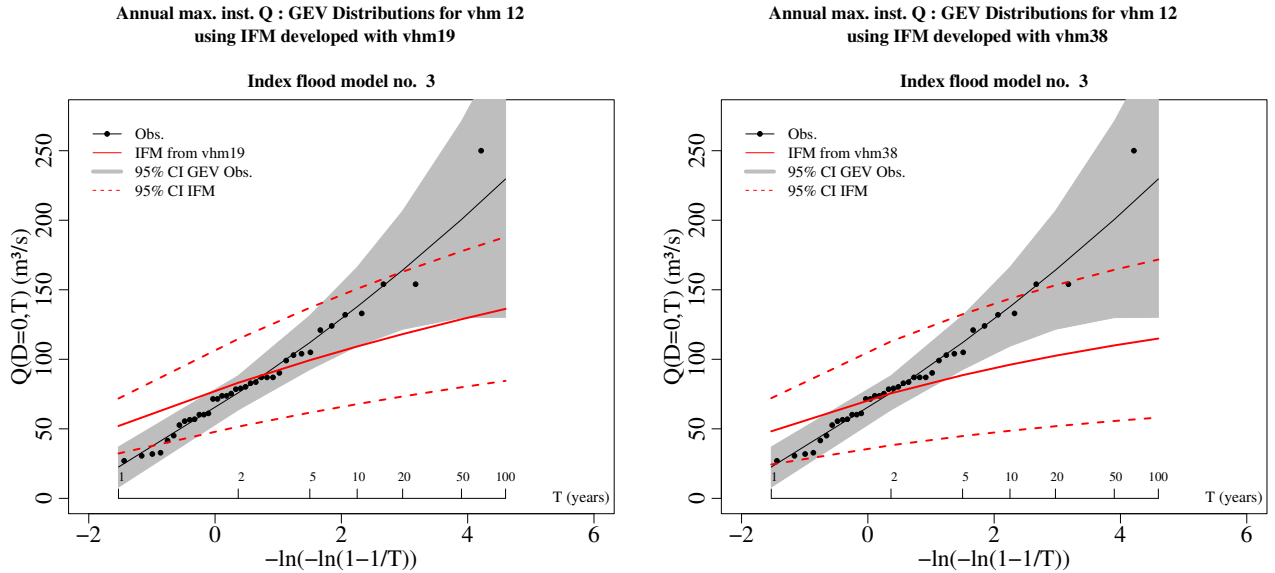


Figure XII.1. Estimation at vhm12 with the IFM developed within vhm19 (left) and within vhm38 (right).

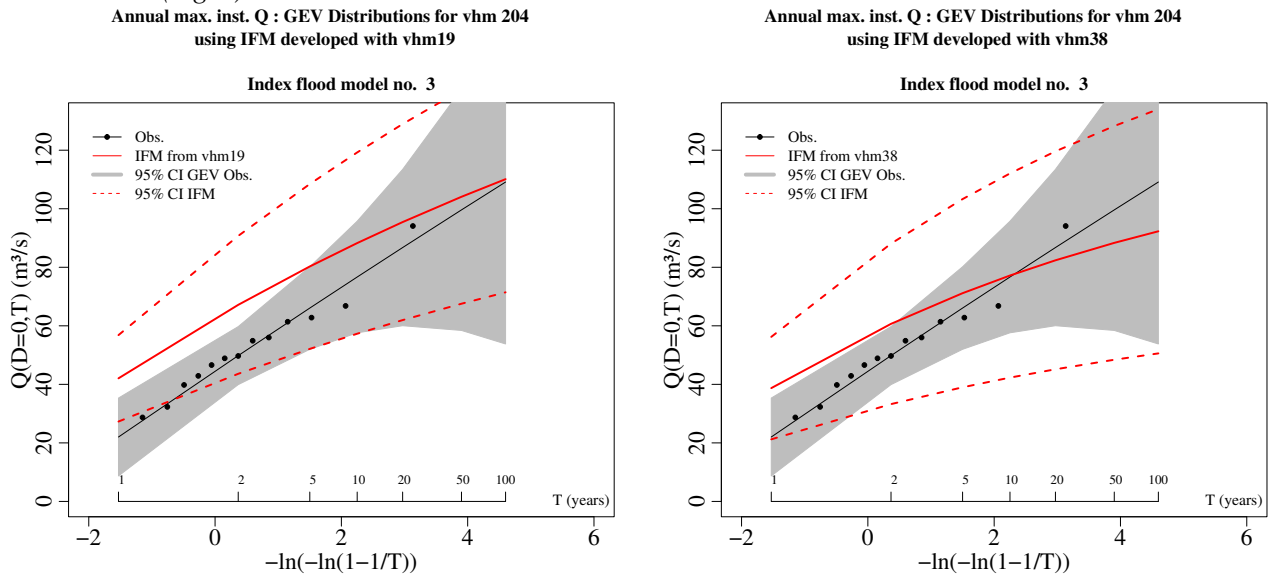


Figure XII.2. Estimation at vhm204 with the IFM developed within vhm19 (left) and within vhm38 (right).

Figure XII: Empirical and modeled instantaneous flood frequency distributions ($Q(D,T)$) for Region 2. Black solid line: reference GEV distribution derived from the observed AMF series. Solid red line: GEV distribution estimated with the IFM ($\hat{Q}_i(D,T) = \hat{\mu}_i(D)q_R(D,T)$ with $\hat{\mu}_i(D) = a(A_iPm_i)^b$) developed using WaSiM simulations and QDF modeling within vhm19 (left) and vhm38 (right). Dashed lines and shaded grey region correspond to the 95% confidence intervals (CI) (see Crochet 2012a). Uncertainties related to hydrological modeling and QDF modeling are not included in the CI calculation (CI IFM in figures legend).

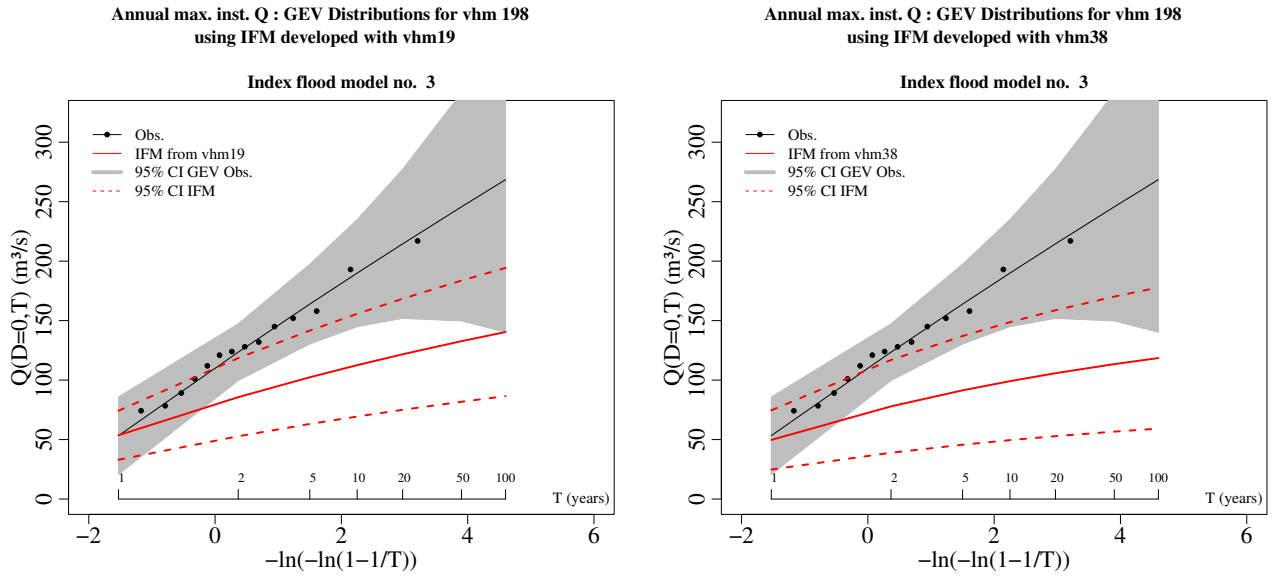


Figure XII.3. Estimation at vhm198 with the IFM developed within vhm19 (left) and within vhm38 (right).

Figure XII: Empirical and modeled instantaneous flood frequency distributions ($Q(D,T)$) for Region 2. Black solid line: reference GEV distribution derived from the observed AMF series. Solid red line: GEV distribution estimated with the IFM ($\hat{Q}_i(D,T) = \hat{\mu}_i(D)q_R(D,T)$ with $\hat{\mu}_i(D) = a(A_i P m_i)^b$) developed using WaSiM simulations and QDF modeling within vhm19 (left) and vhm38 (right). Dashed lines and shaded grey region correspond to the 95% confidence intervals (CI) (see Crochet 2012a). Uncertainties related to hydrological modeling and QDF modeling are not included in the CI calculation (CI IFM in figures legend).